# DEVELOPMENT AND ASSESSMENT OF CARBOXYMETHYL CELLULOSE LOADED ZINC OXIDE NANOPARTICLES FOR ANTIBACTERIAL PROPERTIES

**NIAZ MAHMUD**

**M. ENGINEERING PROJECT**

**DEPARTMENT OF BIOMEDICAL ENGINEERING**
**MILITARY INSTITUTE OF SCIENCE AND TECHNOLOGY**
**DHAKA, BANGLADESH**

**OCTOBER 2024**

# DEVELOPMENT AND ASSESSMENT OF CARBOXYMETHYL CELLULOSE LOADED ZINC OXIDE NANOPARTICLES FOR ANTIBACTERIAL PROPERTIES

NIAZ MAHMUD (SN: 0419260001)

A Project Submitted in Partial Fulfillment of the Requirement for the Degree of Master of Engineering in Biomedical Engineering

DEPARTMENT OF BIOMEDICAL ENGINEERING

MILITARY INSTITUTE OF SCIENCE AND TECHNOLOGY

DHAKA, BANGLADESH

OCTOBER 2024

# DEVELOPMENT AND ASSESSMENT OF CARBOXYMETHYL CELLULOSE LOADED ZINC OXIDE NANOPARTICLES FOR ANTIBACTERIAL PROPERTIES

M. Engineering Project

By

NIAZ MAHMUD (SN.0419260001)

Approved as to style and content by the Board of Examination on 27 October 2024

| | | |
|---|---|---|
| 1. | Lt. Col Md Maruf Hasan, PhD<br>Instructor Class-A<br>Department of Biomedical Engineering<br>Military Institute of Science and Technology (MIST) | _____<br>Supervisor<br>(Chairman) |
| 2. | Col Mohummad Shariful Islam, PSC<br>Senior Instructor and the Head of the Department<br>Department of Biomedical Engineering<br>Military Institute of Science and Technology (MIST) | _____<br>Member<br>(Internal) |
| 3. | Dr. Md. Kaiissar Mannoor<br>Professor<br>Department of Biomedical Engineering<br>Military Institute of Science and Technology (MIST) | _____<br>Member<br>(Internal) |
| 4. | Dr. Md Sharif Hossain<br>Professor<br>Department of Biotechnology and Genetic Engineering<br>Jahangirnagar University | _____<br>Member<br>(External) |

Department of Biomedical Engineering, MIST, Dhaka

DEVELOPMENT AND ASSESSMENT OF CARBOXYMETHYL CELLULOSE LOADED ZINC OXIDE NANOPARTICLES FOR ANTIBACTERIAL PROPERTIES

## DECLARATION

I hereby declare that this project entitled ***"Development and Assessment of Carboxymethyl Cellulose Loaded Zinc Oxide Nanoparticles for Antibacterial Properties"*** is my original work and has been written by me. Furthermore, I have duly acknowledged all the sources of information used in the project. This project has also not been submitted for any degree at any other university.

_____

NIAZ MAHMUD
Student No. 0419260001

October 2024
Department of Biomedical Engineering, MIST, Dhaka

ABSTRACT

**DEVELOPMENT AND ASSESSMENT OF CARBOXYMETHYL CELLULOSE LOADED ZINC OXIDE NANOPARTICLES FOR ANTIBACTERIAL PROPERTIES**

Zinc Oxide (ZnO) Nanoparticles (NPs) have some indigenous properties, which make them a good candidate for versatile biomedical and clinical applications. Although there are numerous potentials, clinical applications of ZnO NPs are still under many obstacles. Due to its stable nature, bigger-sized ZnO has already been used in various clinical applications (i.e., sunscreen, toothpaste, dermatological ointment, anti-etching ointment, etc.). The main problem of using nanosized ZnO in clinical applications is its lack of cell specificity and the tendency to produce reactive oxygen species by external influence (i.e., light, sound, etc.), stability in a biological system. Surface modification of the ZnO NPs can make them more stable, delay or control the release of reactive oxygen species generations, and be cell-specific in biological systems. To make the ZnO NPs enriched with cellulosic properties for antibacterial studies, the surface modification of ZnO NPs has been carried out by Carboxymethyl-Cellulose (CMC), and relevant physical properties (Fourier Transform Infrared Analysis, X-ray Diffraction, Scanning Electron Microscopy, Energy Dispersive X-Ray and Zeta Potentials) have been assessed which confirms the formation of a conjugated matrix of ZnO NPs-CMC. The antibacterial efficacy of the CMC-enriched ZnO NPs was further experimented with over *Lactobacilli (Acidophilus and Bulgaricus)* bacterial species to examine the antibacterial activity against the naïve molecules and found that with a slight modification of ZnO treated by CMC causes an overall increase in antibacterial efficacy at a concentration (mass/liquid-volume) of 0.5% (w/v) (viability reduction: 51% vs 66 %) & 1.5% w/v (viability reduction: 63 % vs 77 %) and insignificant at deficient concentrations (0.1% w/v) for both.

**Key Words:** Zinc Oxide Nanoparticles (ZnO NPs), Carboxymethyl Cellulose (CMC), Surface Modification, Controlled Release, Antibacterial.

# সারসংক্ষেপ

## DEVELOPMENT AND ASSESSMENT OF CARBOXYMETHYL CELLULOSE-LOADED ZINC OXIDE NANOPARTICLES FOR ANTIBACTERIAL PROPERTIES

জিঙ্ক অক্সাইড ন্যানো পার্টিকেলগুলির কিছু অসাধারন বৈশিষ্ট্য রয়েছে, যা তাদের বহুমুখী বায়োমেডিকাল এবং ক্লিনিকাল অ্যাপ্লিকেশনের জন্য একটি ভাল প্রার্থী করে তুলতে পারে। যদিও অসংখ্য সম্ভাবনা, জিঙ্ক অক্সাইড ন্যানো পার্টিকেলগুলির ক্লিনিকাল অ্যাপ্লিকেশনগুলি এখনও অনেক বাধার মধ্যে রয়েছে। স্থিতিশীল প্রকৃতির কারণে বড় আকারের জিঙ্ক অক্সাইড ইতিমধ্যেই বিভিন্ন ক্লিনিকাল অ্যাপ্লিকেশনে ব্যবহার করা হয়েছে (যেমন, সানস্ক্রিন, টুথপেস্ট, চর্মরোগ সংক্রান্ত মলম, অ্যান্টি-এচিং মলম ইত্যাদি)। ক্লিনিকাল অ্যাপ্লিকেশনগুলিতে ন্যানোসাইজড জিঙ্ক অক্সাইড ব্যবহার করার প্রধান সমস্যা হল কোষের নির্দিষ্টতার অভাব, এবং বাহ্যিক প্রভাব (যেমন আলো, শব্দ, ইত্যাদি) দ্বারা প্রতিক্রিয়াশীল অক্সিজেন প্রজাতি তৈরি করার প্রবণতা, একটি জৈবিক ব্যবস্থায় স্থিতিশীলতা। জিঙ্ক অক্সাইড ন্যানো পার্টিকেলগুলির পৃষ্ঠের পরিবর্তন এটিকে আরও স্থিতিশীল করে তুলতে পারে, প্রতিক্রিয়াশীল অক্সিজেন প্রজাতির প্রজন্মের মুক্তিকে বিলম্বিত বা নিয়ন্ত্রণ করতে পারে এবং জৈবিক ব্যবস্থায় কোষ-নির্দিষ্ট হতে পারে। অ্যান্টিব্যাকটেরিয়াল অধ্যয়নের জন্য জিঙ্ক অক্সাইড ন্যানো পার্টিকেলগুলির কে সেলুলোসিক বৈশিষ্ট্য দিয়ে সমৃদ্ধ করার জন্য, জিঙ্ক অক্সাইড ন্যানো পার্টিকেল-এর পৃষ্ঠের পরিবর্তন কার্বোক্সিমিথাইল-সেলুলোজ দ্বারা করা হয়েছে এবং প্রাসঙ্গিক ভৌত বৈশিষ্ট্যগুলি (ফুরিয়ার ট্রান্সফ্রম ইনফ্রারেড এনালাইসিস, এক্সরে ডিফ্রাকশন, স্ক্যানিং ইলেক্ট্রন মাইক্রোস্কোপি , এনার্জি ডিস্পারসিভ এক্সরে এবং জেটা পটেনশিয়াল) করা হয়েছে। মূল্যায়ন করা হয়েছে যা জিঙ্ক অক্সাইড ন্যানো পার্টিকেল-কার্বোক্সিমিথাইল-সেলুলোজ এর একটি সংযোজিত ম্যাট্রিক্স গঠন নিশ্চিত করে। কার্বোক্সিমিথাইল-সেলুলোজ-সমৃদ্ধ জিঙ্ক অক্সাইড ন্যানো পার্টিকেল-এর অ্যান্টিব্যাকটেরিয়াল কার্যকারিতা ল্যাকটোব্যাসিলি (অ্যাসিডোফিলাস এবং বুলগারিকাস) ব্যাকটেরিয়া প্রজাতির উপর পরীক্ষা করা হয়েছে এবং দেখা গিয়েছে যে কার্বোক্সিমিথাইল-সেলুলোজ দ্বারা পৃষ্ঠ জিঙ্ক অক্সাইড ন্যানো পার্টিকেলগুলির -এর সামান্য পরিবর্তনের ফলে সামগ্রিকভাবে অ্যান্টিব্যাকটেরিয়াল বৃদ্ধি ঘটে। সামগ্রীক ভাবে দেখা যায়, 0.৫% w/v এর ঘনত্বে কার্যকারিতা (কার্যযোগ্যতা হ্রাস: ৫১% বনাম ৬৬%) এবং ১.৫% w/v (কার্যযোগ্যতা হ্রাস: ৬৩% বনাম ৭৭%) অ্যান্টিব্যাকটেরিয়াল ধর্ম মোটামুটি উল্লেখ্য এবং উভয়ের জন্য-ই খুব কম ঘনত্বে (0.১% w/v) অ্যান্টিব্যাকটেরিয়াল ধর্ম অনেকটাই নগণ্য.

## ACKNOWLEDGEMENTS

First, I would like to thank the most gracious and merciful Almighty Allah for showering blessings and guidance throughout my project work, giving me the strength to pursue the M. Engineering degree, and allowing me to complete this project successfully.

Then, we would like to acknowledge my deep gratitude to the oral examination committee members and their guidance truly helped me enhance the quality of this dissertation writing.

It is an immense pleasure to convey my deepest gratitude towards my supervisor, **Lieutenant Colonel Md Maruf Hasan, PhD,** Associate Professor of the Department of Biomedical Engineering, MIST; thanks to him for his invaluable guidance, suggestions, energy, patience, and inspiration. This thesis would never have been done without his help and dedication at every step of this journey. Each meeting has been a wealth of information, and I have had a great time learning new things. To express my gratitude for his unfailing support, my supervisor deserves another word of thanks.

I want to thank the respected Head of the Department, **Colonel Mohummad Shariful Islam** for providing guidance and support. I must acknowledge the guidelines of **Assistant Professor Dr. Md. Asadur Rahman** of the BME department to improve the writing of this dissertation. I want to thank all faculty members of the Department of Biomedical Engineering, MIST, for their unwavering support and assistance during this project. I would also like to thank other office staff for their help.

Finally, I must acknowledge the support of my family members, especially my parents, **Md. Abdul Jalil** and **Nasrin Akter**, thank you for your continuous motivation and support.

Author

## TABLE OF CONTENTS

## LIST OF FIGURES

## LIST OF TABLES

## LIST OF ABBREVIATIONS

| | |
|---|---|
| AAPS | American Association of Pharmaceutical Sciences |
| ACS | American Chemical Society |
| AIDS | Acquired Immune Deficiency syndrome |
| BAEC | Bangladesh Atomic Energy Commission |
| CFU | Colony Forming Unit |
| CMC | Carboxymethyl Cellulose |
| COA | Certificate of Analysis |
| DM | Demineralized |
| DNA | Deoxy ribonucleic acid |
| EDX | Energy Dispersive X-Ray |
| EMA | European Medicinal Agency |
| FDA | Food and Drugs Administration |
| FTIR | Fourier Transform Infrared |
| GMP | Good Manufacturing Practice |
| GNP | Gold Nano-particles |
| GPTMS | (3-glycidoxypropyl)-trimeth-oxysilane |
| HMMC | 1-(3-Hydroxy-4-methoxyphenyl)-2-(methylamino) |
| IL | Interleukins |
| IR | Infrared |
| ISO | International Standardized Organization |
| KV | Kilovolts |
| MIST | Military Institute of Science and Technology |
| MRS | Man–Rogosa–Sharpe agar |
| MS | Mass spectroscopy |
| NCBI | National Center for Biotechnology Information |
| NPs | Nanoparticles |
| PBS | Phosphate Buffer Saline |
| PDA | Parenteral Drug Association |
| PEG | Poly Ethylene Glycol |

| | |
|---|---|
| PVA | Poly Vinyl Alcohol |
| RNA | Ribonucleic Acid |
| ROS | Reactive oxygen Species |
| SEM | Scanning Electron Microscope |
| TNF | Tumor Necrosis Factor |
| UV | Ultraviolet |
| WHO | World Health Organization |
| XRD | X-ray Diffraction |
| ZNO | ZnO |

# CHAPTER 1
# INTRODUCTION

## 1.1 Background of the Study

Bacterial disease contributes to significant global morbidity. In a study by the Lancet, there were around 7.7 million deaths in 2019 from 33 bacterial pathogens (Ikuta *et al.*, 2022). Usually, in most studies, the scientific community focuses on pathogenic strains when it comes to bacterial infection. However, even non-pathogenic bacteria could be deadly among vulnerable groups (Pigłowski, 2019). For example, commensal lactobacillus can cause cytolytic vaginosis, dysbiosis, endocarditis, or rarely gastric cancer among immunosuppressed patients with HIV, diabetic, or geriatric groups (Antoun *et al.*, 2020). Although numerous antibiotics are used to overcome infections, they are not free from side effects, and there are chances of antimicrobial resistance. Conventional antibiotics primarily inhibit DNA and RNA synthesis, cell wall rupture, or bacterial metabolism (Reygaert, 2018). Besides traditional antibiotics, many nanoparticles are effective against bacteria (Aflakian *et al.*, 2023). They mainly work by producing reactive oxygen species derivatives and metallic ions and blocking the internal kinetics of bacterial metabolic pathways (Makabenta *et al.*, 2021). Copper, zinc, nickel, and silver have already been assessed in many studies for active antibacterial potentialities (Makabenta *et al.*, 2021; Aflakian *et al.*, 2023). Among NPs, ZnO is famous for its low toxicity and applications in pharmaceutical products (Mendes *et al.*, 2022). For example, bigger-sized ZnO is the active ingredient of anti-itching ointment. Moreover, smaller-sized zinc oxide is a proven antibacterial agent that works by producing reactive oxygen species that destroy cells, releasing metallic zinc ions that block gene expression and intracellular outflux (Mendes *et al.*, 2022).

## 1.2 Problem Statements

Nanomaterial has some intrinsic properties (large surface area, surface plasmonic property, penetration capacity, interactions with external fields, i.e., light, magnet, sound wave, etc.), which makes them very promising for biomedical and clinical applications(Anik, Mahmud,

Al Masud, *et al.*, 2022). Although the giant-sized molecules might already be used in clinical applications (i.e., ZnO), the properties of smaller or nano-scaled sizes of the same molecule could have very different properties that can be utilized in versatile applications. For example, ZnO treats or prevents minor skin irritations such as burns, cuts, and diaper rash. It may be used as a sunscreen due to its ultraviolet (UV) blocking capacity (Gupta *et al.*, 2014). On the other hand, nano-scaled ZnO has some indigenous properties (i.e., tendency to produce reactive oxygen species or oxidative stress, intracellular penetration, and interfering with UV) which can be utilized in treating diseases caused by bacterial, viral, fungal, or protozoal infections, cancer. NPs can also be used to diagnose diseases (Mandal, 2016a). Unfortunately, till now, nano-particles couldn't be used directly in clinical applications as the scientific community couldn't rule out the chances of risk outweighing benefits (Wolfram *et al.*, 2015). Despite the numerous possibilities, ZnO has not yet gained popularity in clinical applications due to its inherent toxicity, instability, and lack of cell-specific permeability (Jiang, Pi and Cai, 2018). Surface modification could resolve the existing limitations to a certain degree, making the nano ZnO more regulated and stable in a biological environment (Luo *et al.*, 2014). In some studies, we have found that organic polymers like carboxymethyl cellulose can stabilize nanoparticles and increase their antibacterial effect (Khalaf *et al.*, 2021). This study will also observe whether similar loading over zinc oxide could show higher potentiality than naïve zinc oxide.

### 1.3 Objectives of the Project

The objectives of this project:

- To develop carboxymethyl cellulose-loaded ZnO NPs.
- To characterize the loaded ZnO NPs compared to control substances using Fourier transform infrared spectroscopy (FTIR), X-ray diffraction (XRD), Scanning electron microscope (SEM), and Energy dispersive X-ray analysis (EDX).
- To assess the stability of CMC loaded ZnO NPs in comparison to naïve ZnO NPs.
- To assess the antimicrobial activity of ZnO NPs against *Lactobacillus* species.

## 1.4 Motivation of the Project

Infectious diseases caused by pathogens (Bacterial, Viral, fungi, etc.) and aging disease (i.e. Cancer) kill millions of people every year. Although many antibiotics exist to overcome bacterial diseases, antibiotic resistance is already a big issue and will be a big concern for the next generations. Innovations in new drugs, targeted delivery, and reducing the toxicity of existing drugs are urgently required. In this study, the surface property of ZnO NPs has been modified by carboxymethyl cellulose, which should make ZnO NPs more stable and more targeted to bacterial cells. CMC may facilitate the conjugation of ZnO NPs with other drugs, such as antimicrobial peptides and chemotherapeutics.

## 1.5 Organization of the Project

The project structure comprises five chapters: chapter 1: Introduction, chapter 2: Literature Review, chapter 3: Experimental Procedure, chapter 4: Results and Discussion, and Chapter 5: Conclusion and Recommendation for Future Study. The details of the organization of the thesis are as follows:

**Chapter 1 (Introduction)** comprises an introduction to the project topic and the background behind the research. Also, the motivation and objectives of the thesis have been included in this chapter. Finally, the chapter concludes with a mention of the structure or organization of the thesis in this book.

**Chapter 2 (Literature Review)** consists of the theoretical studies required for the project work. It describes details of nanoparticles, clinical applications, existing barriers, ways to resolve them, etc.

**Chapter 3 (Experimental Procedure)** describes the project methods and materials. This chapter includes the name of the materials used in the project, the preparation method of conjugating CMC with ZnO NPs, and physicochemical characterization methods compared to the control substance (i.e., Fourier Transform Infrared Spectroscopy-FTIR, X-ray Diffraction-XRD, Scanning Electron Microscopy-SEM, Energy Dispersive X-Ray-EDX and Zeta Potentials) and biological evaluation (e.g., antimicrobial activity assessment over a selective bacterial species).

**Chapter 4 (Results and Discussion)** provides the project work's outcomes and observations and discusses the significance of the experiments and the relative contributions of the work to the field of study. The outcomes and observations have been displayed in graphs and tables where required.

**Chapter 5 (Conclusions and Future Recommendation of the Study)** concludes the project and summarizes its output and findings. It also provides recommendations for further study, inspiring future researchers to build on this work and continue fighting against bacterial diseases.

# CHAPTER 2
# LITERATURE REVIEW

The potential use of NPs for treatment, diagnostics, and several other medical purposes has been under consideration for a long time due to their unique characteristics, such as surface characteristics, plasmonic properties, and light and radiation accumulation properties (Anik, Mahmud, Al Masud, *et al.*, 2022; Mahmud *et al.*, 2022) ZnO NPs have long been studied for their antimicrobial and other therapeutic potency, but how they work in different species remains a matter of research. Because of their abundance and availability, ZnO NPs are an excellent candidate for future nanotherapeutics. ZnO is the second most available metal oxide after iron oxide (Lakshmipriya and Gopinath, 2021). Due to its availability, economic benefits, and some Indigenous physical and chemical properties (i.e., biocompatibility, low toxicity, high UV-absorption tendency, antimicrobial tendency, and cytotoxic effect against cancer cells), ZnO has long been considered a good candidate for biomedical and pharmaceutical applications (Wisz *et al.*, 2017). Many drug regulatory authorities have approved ZnO for antibacterial creams, lotions, ointments, mouthwashes, and paints as antimicrobial agents and in surface coatings as biofilm growth inhibitors. However, these are not Nano-sized ZnO (Mandal, 2016b). The antimicrobial activity of ZnO NPs is critically dependent on NP size and shape (Babayevska *et al.*, 2022). Multiple scientific studies have supported the post that ZnO penetrates the cell membrane and triggers ROS-oxidation of the cellular contents, promoting cell death (Cotton *et al.*, 2019; Anik, Mahmud, Masud, *et al.*, 2022). ZnO NPs enter the cellular membrane via a diffusion mechanism, which disintegrates the membrane and accumulates in the cytoplasm, interacting with biomolecules, causing cell apoptosis and leading to cell death (Siddiqi *et al.*, 2018).

ZnO NPs have an indigenous property to produce ROS included in biological systems (Murali *et al.*, 2021). The endocytosis mechanism readily absorbs ZnO NPs by cellular membranes and quickly breaks down into $Zn^{+2}$ ions (Murali *et al.*, 2021). Because of their semiconductor structure and surface imperfections (Wisz *et al.*, 2017), ZnO NPs yield more ROS when exposed to light/waves, giving them more excellent catalytic capabilities (Racca *et al.*, 2020). Under oxidative damage to bacterial membranes and DNA, ROS

molecules such as hydrogen peroxide ($H_2O_2$), singlet oxygen ($^1O_2$), superoxide anions ($O_2\bullet-$), and hydroxyl radicals (•OH) are vital to antibacterial activities (Lakshmi Prasanna and Vijayaraghavan, 2015). Furthermore, the zinc ions ($Zn^{+2}$) that are liberated from ZnO NPs are crucial for controlling biological processes and inhibiting the growth of bacteria (Wang *et al.*, 2023). However, the wavelength range and intensity of the external light determine the photocatalytic activity of ZnO NPs (Hwang *et al.*, 2022). In **Figure 2.1**, the transformation mechanism of ZnO NPs to $Zn^{+2}$ molecules and ROS derivatives ($O_3^-$, $H_2O_2$, $OH^-$ etc.) has been depicted (Isık, Hilal and Horzum, 2019a; Liao *et al.*, 2020). From **Figure 2.2(a), Figure 2.2(b), Figure 2.3,** and **Figure 2.4**, the process of autophagic / mitophagy cell death, oxidative DNA damage, cell cycle arrest, necrosis, and extrinsic apoptosis due to the impact of $Zn^{+2}$ molecules and ROS derivatives ($O_3^-$, $H_2O_2$, $OH^-$ etc.) has been depicted as per literature (Sharma, Anderson and Dhawan, 2012; Hwang *et al.*, 2022). Despite numerous benefits in in-vivo experiments, using ZnO NPs is still challenging, and many barriers must be overcome to complement the benefits. Despite the successful application of large-sized ZnO in several clinical products—such as sunscreens, toothpaste, dermatological ointments, and anti-itching treatments—there are notable challenges associated with using ZnO NPs in medical settings. One of the main concerns is their lack of cell specificity, which means that ZnO NPs can interact with various cell types rather than selectively targeting specific cells (Liao *et al.*, 2020). This non-specific behavior can lead to unintended effects on healthy tissues. Another significant drawback is the absence of an effective reactive oxygen species (ROS) triggering agent. ROS can play a vital role in various therapeutic applications, especially in targeted therapies that require the generation of oxidative stress to eliminate diseased cells (Afzal *et al.*, 2023). Without a proper trigger, the efficacy of ZnO NPs in these contexts may be compromised. Finally, the stability of ZnO NPs in liquid dispersants poses another issue (Navas *et al.*, 2020). The tendency of these nanoparticles to aggregate or settle can limit their effectiveness and reduce their overall penetration depth when exposed to external light, which is often necessary for activating their therapeutic properties (Navas *et al.*, 2020). These factors collectively hinder the full potential of ZnO NPs in clinical applications, necessitating further research and development to enhance their specificity, activation mechanisms, and stability (Hwang *et al.*, 2022). Even if appropriately activated by external

influence (i.e., light, shock wave, etc.)(Bogdan, Pławińska-Czarnak and Zarzyńska, 2017; Racca *et al.*, 2020), ZnO NPs medicated ROS not only causes harm to the targeted pathogen but also causes harm to a certain degree to healthy mammalian cells due to lack of cell specificity (unless designed in a targeted way) which possess the risk of inflammation, tissue damage, and genotoxicity (Rasmussen *et al.*, 2010). The process of damaging healthy mammalian cells by $Zn^{+2}$ molecules and ROS derivatives ($O_3^-$, $H_2O_2$, $OH^-$ etc.) has been depicted in **Figure 2.3**.

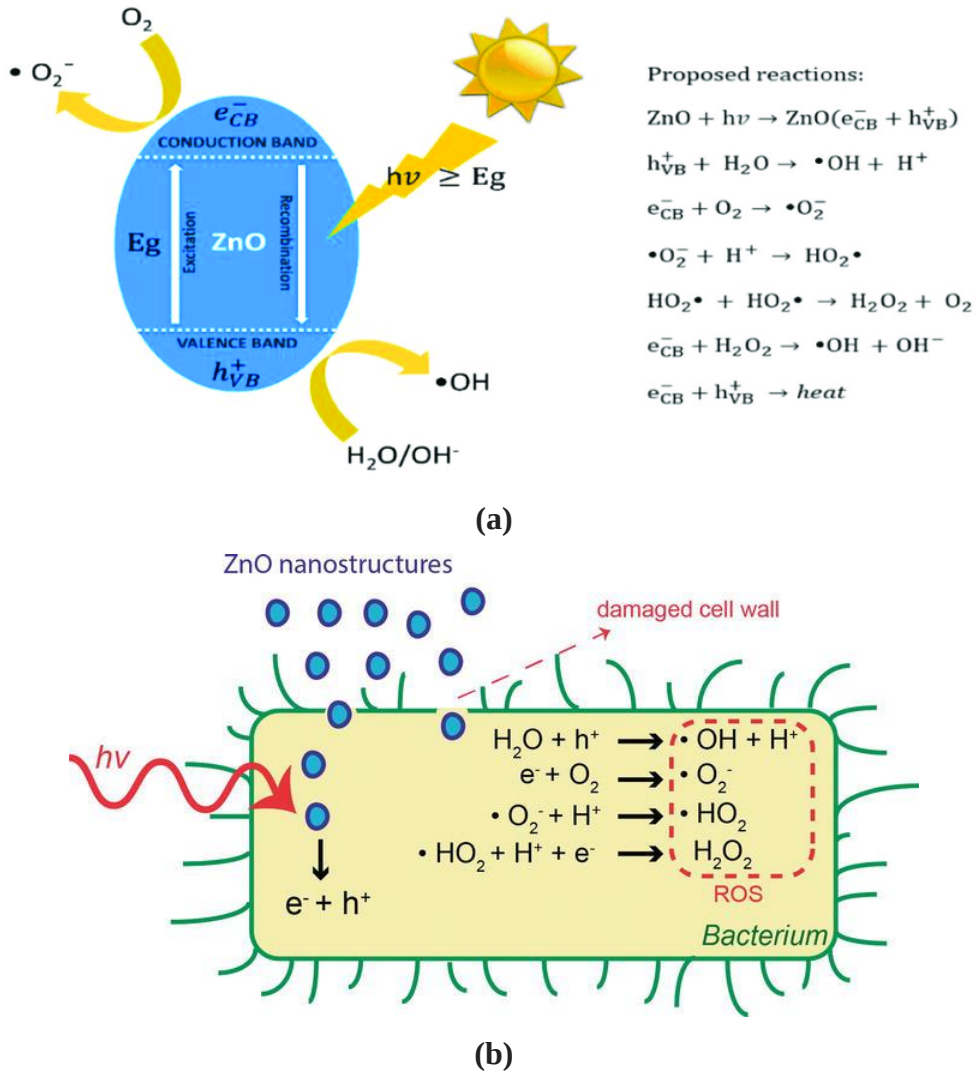


**Figure 2.1:** (a) ROS generation from ZnO NPs. Reprinted with permission from (Liao *et al.*, 2020), Copyright MDPI. (b) Generation of ROS from ZnO NPs intracellularly upon exposure to light. Reprinted with permission from (Isık, Hilal, and Horzum, 2019), *Copyright MDPI.*

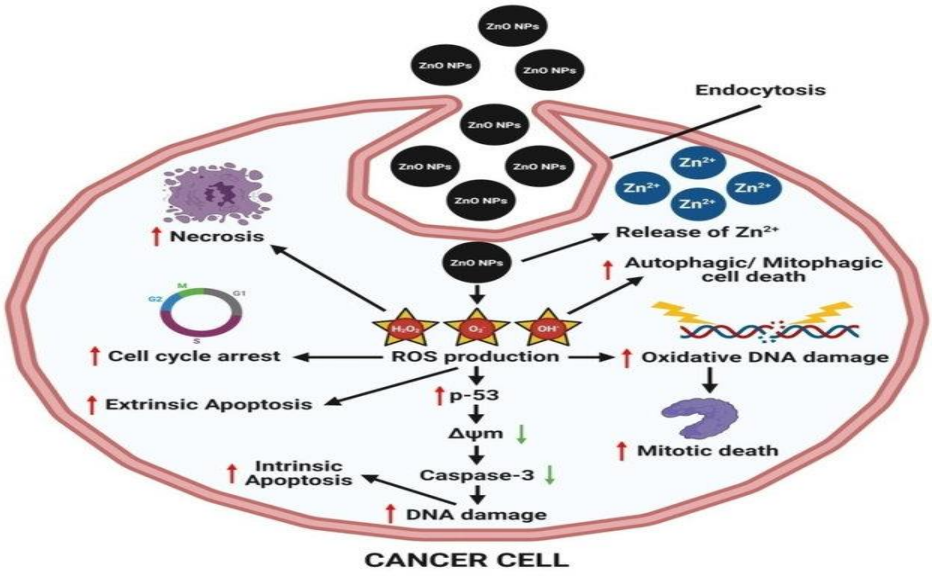


**(a)**

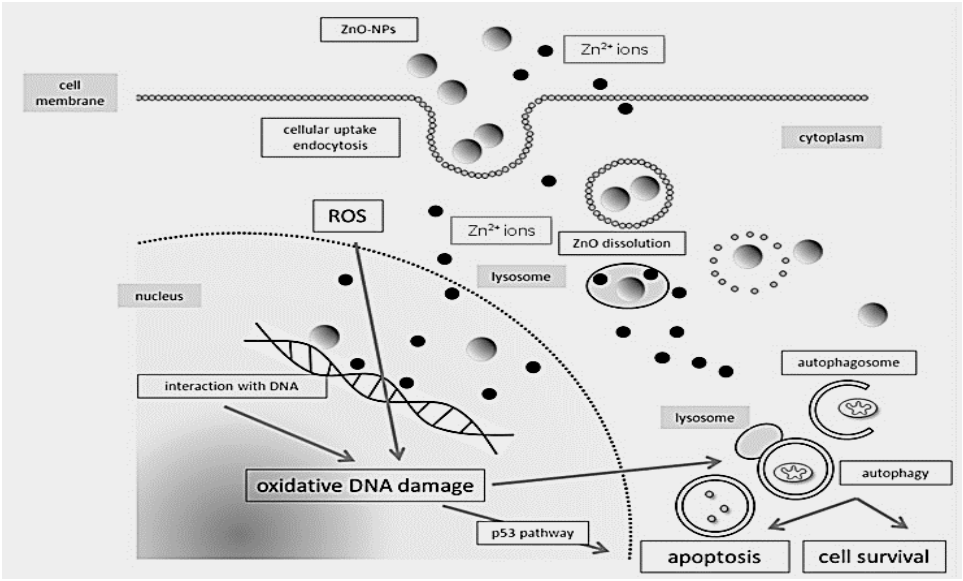


**(b)**

**Figure 2.2:** (a) Possible anticancer mechanism of ZnO NPs. Reprinted with permission from (Murali *et al.*, 2021). Copyright MDPI (b) A hypothetical model of ZnO NPs -induced genotoxicity to Mammalian Cell. Reprinted with permission from (Scherzad *et al.*, 2017), *Copyright MDPI.*

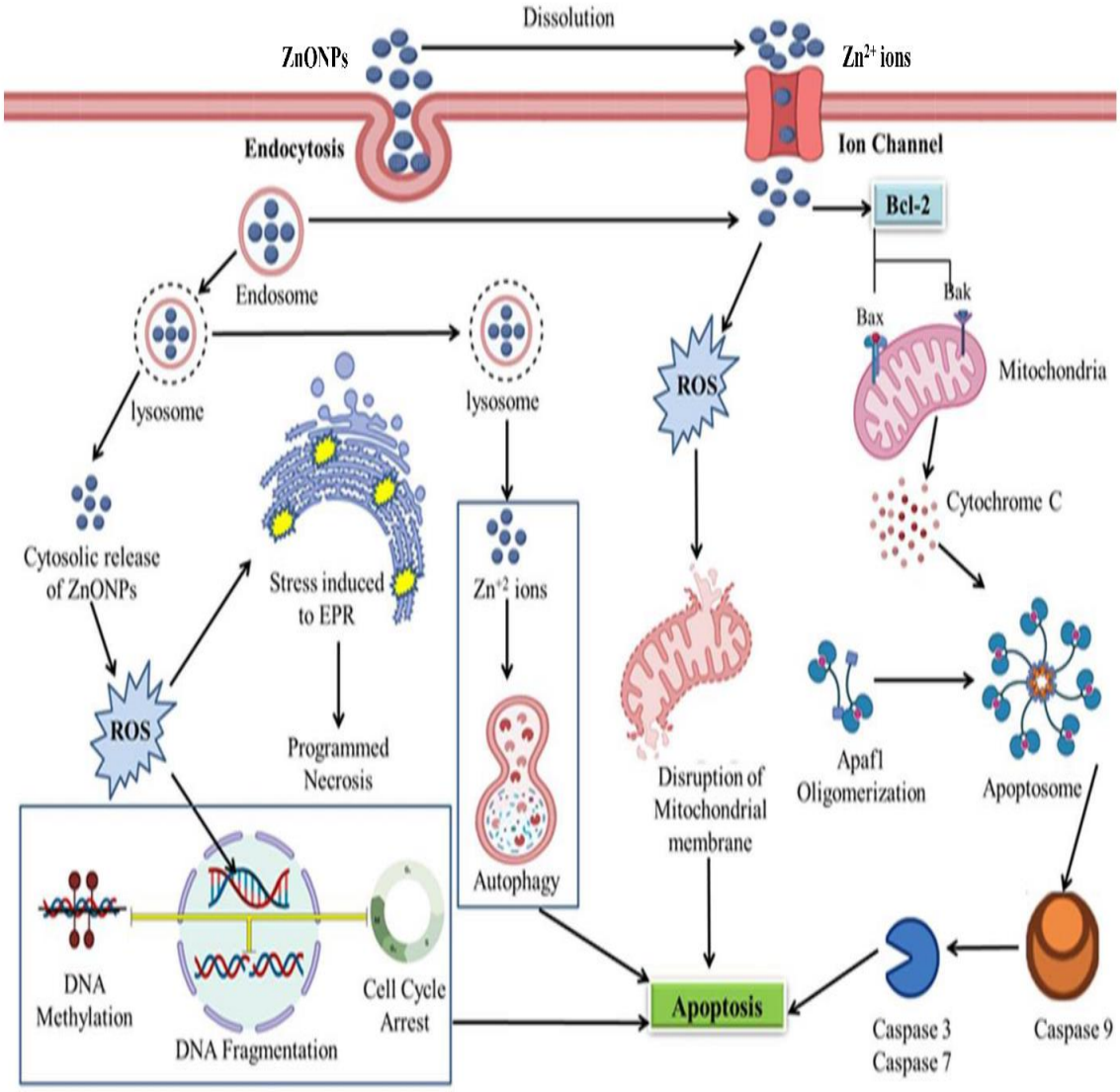


**Figure 2.2:** The mechanism of entry of ZnO NPs into Mammalian Cells by endocytosis and the formation of $Zn^{+2}$ ultimately influences ROS. Reprinted with permission from (Anjum *et al.*, 2021). Copyright MDPI.

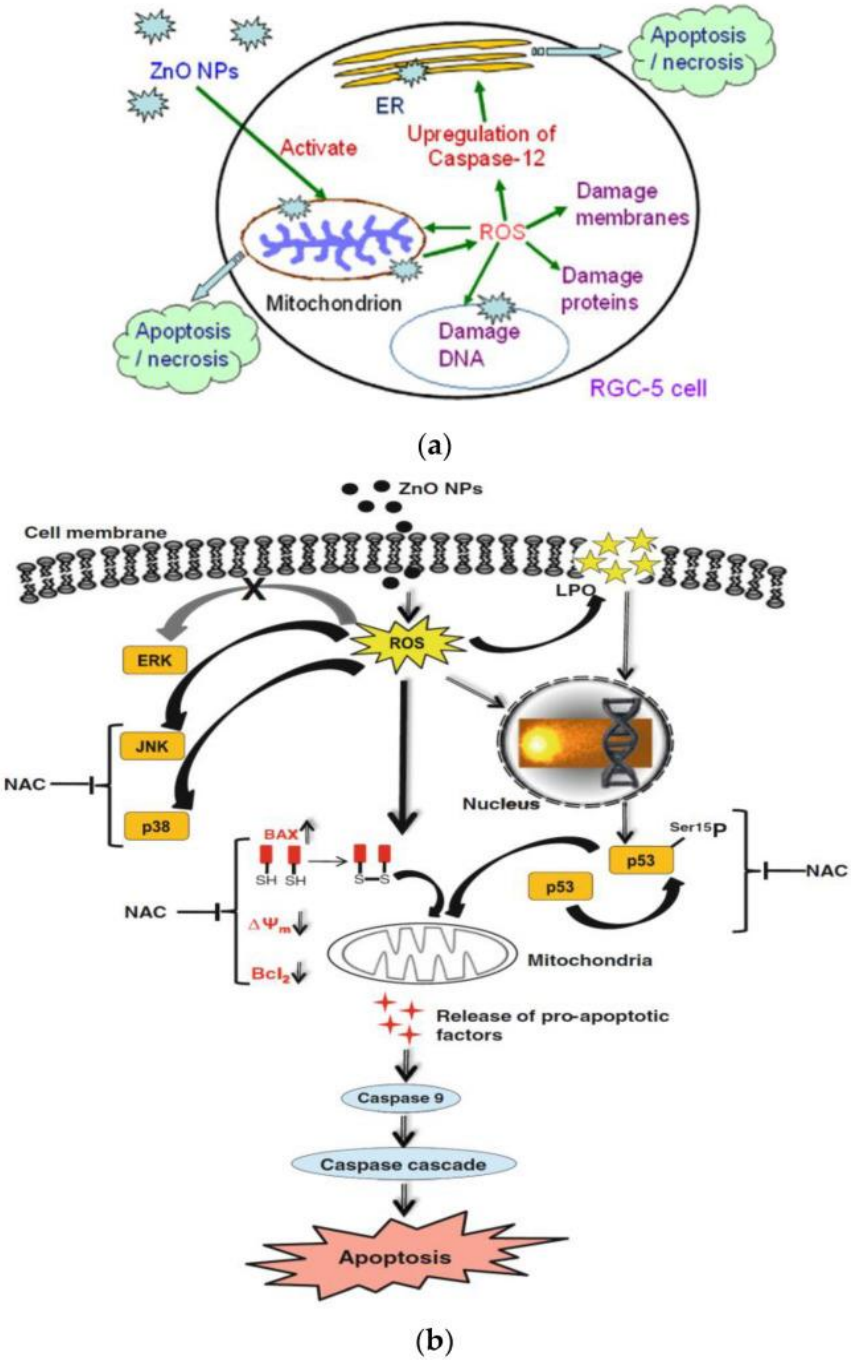


**Figure 2.3:** (a) ZnO NPs -induced apoptosis/necrosis of retinal ganglion cell. Reprinted with permission from (Guo *et al.*, 2013). *Copyright Elsevier* (b) Mechanisms responsible for ZnO NPs mediated toxicity and apoptosis in human liver cells. N-acetyl cysteine (NAC) effectively inhibits BCL2-associated protein (Bax) induction and p53 phosphorylation. Reprinted with permission from (Sharma, Anderson and Dhawan, 2012), *Copyright Springer.*

As a conventional wide bandgap semiconductor with superior biocompatibility, safety, and long-term efficacy over other antibacterial materials, ZnO NPs are well-suited for various biomedical and pharmaceutical applications. ZnO NPs have demonstrated significant bactericidal activity against Gram-positive and Gram-negative bacteria, including Escherichia coli, Staphylococcus aureus, Pseudomonas aeruginosa, and Klebsiella pneumonia. (Jiang, Lin and Cai, 2020; Li, Liao and Tjong, 2020). The antibacterial mechanism of ZnO NPs can be classified into three different mechanisms: (a) generation of ROS, (b) $Zn^{+2}$ induced damage, and (c) Interaction of ZnO NPs with the cell membrane by membrane dysfunction or cell internalization (Jiang, Lin and Cai, 2020).

A few critical factors, such as toxicity, cellular uptake, dispersion stability in biological systems, stability, biocompatibility, and the capacity of NPs to be absorbed by target cells in contrast to non-target cells, should be considered when using any NPs in clinical applications (e.g., antibacterial or anticancer). ZnO is considered insoluble in water but readily soluble in acidic solutions with pH values between two and four (Avramescu *et al.*, 2017; Cardoso *et al.*, 2021). Another crucial aspect to consider is whether the $Zn^{+2}$ released from the ZnO NPs remained in their ionized state or if they were re-formed into the crystalline phase with the abundant ligand molecules in the body. ZnO NPs may be internalized by cells in their particle form and fully dissolve within the cells (Gilbert *et al.*, 2012). This process leads to the formation of intracellular $Zn^{+2}$ ions bound to molecular ligands, which is confirmed by high-resolution X-ray spectroscopy and high-element-sensitivity X-ray microprobe investigation (Gilbert *et al.*, 2012). Conversely, production methods, such as heating, cooling, mixing, and coating, can also impact the destiny of nanoparticles, either by altering their structure or causing them to break down (Youn and Choi, 2022). ZnO NPs have been reported to be modified to improve their chemical and physical properties, which has resulted in excellent clinical efficacy. **Table 2.1**, summarizes the previous studies performed between 2015-2023 (based on the NCBI PubMed search database) on surface modification of ZnO NPs by external agents and outcomes of the antibacterial activity by the conjugation.

**Table 2.1:** Summarized Studies of Surface Modification of ZnO NPs by External Agents and Outcomes.

| Application Objectives | Modifying Agent | Outcome of Surface Modification | Reference |
|---|---|---|---|
| Improving Antibacterial Efficacy | Addition of (3-glycidyloxypropyl) trimeth-oxysilane (GPTMS) with ZnO NPs. | 5 nm ZnO NP modified by GPTMS has excellent potential for use as an inorganic antibacterial material. | (Lallo da Silva *et al.*, 2019) |
| Improving Catalytic and Antibacterial Efficacy | The surface modification of spherical ZnO with Ag nanoparticles | The Ag-modified ZnO NPs exhibited enhanced catalytic activity towards organic pollutants and antibacterial efficacy against K. pneumoniae, S. Typhimurium, P. vulgaris, S. mitis, and S. faecalis. They performed better than the pure ZnO NPs under UV and sunlight irradiations. | (Fouladi-Fard *et al.*, 2022) |
| Antialgal and Anti-yeast Applications | Zinc sulfide (ZnS), silica (SiO2), poly (sodium 4-styrene sulfonate) sodium salt (PSS), and poly (allylamine hydrochloride) (PAH) polyelectrolytes coated ZnO NPs. | The effect of the ZnO NPs surface coating was much stronger bactericidal than the ROS effect due to illumination with UV light.<br><br>This suggests that the antibacterial activity of the NPs is significantly more dependent on their adhesion to the microbial cell wall than on the production of ROS alone. | (Halbus, Horozov and Paunov, 2020) |
| Enhancement of NP stability in Aqueous solutions. | Surface Modification of the ZnO NPs with γ-Amino-propyl-tri-ethoxy-silane (APTES) | Visual dispersion stability tests demonstrated that APTES-grafted ZnO NPs had become more stable in aqueous solution than non-modified ZnO NPs | (Rabin *et al.*, 2015) |
| Improving Antibacterial Efficacy | ZnO NPs with Lysozyme Modification (LY-ZnO). | LY-ZnO NPs had more excellent antibacterial activity than ZnO. | (Yuan *et al.*, 2021) |

| | | | |
|---|---|---|---|
| Improving Antibacterial Efficacy | ZnO NPs surface modification employing dido-decyl-dimethylammonium bromide (DDAB) as a cationic surfactant | The sedimentation test findings showed that compared to pure ZnO NPs, the SM-ZnO NPs showed higher dispersion and less aggregation. Because of the SM-ZnO NPs' high surface positive charge, the bacteria were exposed to more $Zn^{+2}$, which had a greater surface tendency. | (Viswanathan *et al.*, 2020) |
| Improving Antibacterial Efficacy | Polydopamine (PDA)-Based Surface Modification of ZnO NPs on Sericin/Polyvinyl Alcohol (SS/PVA) Composite Film. | The ZnO NPs-PDA-SS/PVA composite film exhibited improved antimicrobial action against Staphylococcus aureus and Escherichia coli. | (Ai *et al.*, 2019) |
| Improving surface characteristics to control marine toxicity | ZnO-NPs (20 nm) were coated with 3-amino-propyltrimethoxysilane (A-ZnO-NPs). | It provides the ZnO NPs with a more hydrophilic surface, which turns the particles hydrophobic. This hinders the instant generation of ROS. | (Yung *et al.*, 2017) |
| Improving Antibacterial Efficacy | Surface-Modified Copper Doped ZnO NPs (Cu: ZnO NPs) | Surface-modified copper-doped Cu: ZnO NPs have significant potential for their usefulness as antibacterial agents. | (Khalid *et al.*, 2021) |

The interaction of a correctly modified NP's surface with a molecular target overexpressed by cells and tissues is the basis for actively using NPs to target medications and contrast agents (Yoo *et al.*, 2019). The compounds that alter the surface of NPs include aptamers, oligosaccharides, peptides, small proteins, and antibodies (Large *et al.*, 2019). It is frequently required to biochemically modify the NP surface with these particular targeting ligands to increase their stability in biological fluids and decrease toxicity (as is commonly the case with silver NPs)(Guerrini, Alvarez-Puebla and Pazos-Perez, 2018; Borowik *et al.*, 2019). Scanning electron microscopy (SEM), Fourier transform infrared spectroscopy (FTIR), X-ray diffraction (XRD), Energy Dispersive X-ray (EDX), and Zeta (ζ-potential)

analysis are some of the most valuable and simple techniques used to study shape, size, chemical composition, and superficial charge of NPs (Sanità, Carrese and Lamberti, 2020).

The pharmaceutical, medical, papermaking, textile, and other industries have all embraced cellulosic materials for different purposes because of their numerous appealing qualities, which include outstanding thermal and chemical stability, non-toxicity, excellent biocompatibility, and biodegradability (Pandey *et al.*, 2012; Altomare *et al.*, 2016). Among them, CMC (The structural visualization of CMC shown in **Figure 2.5**) is a water-soluble polymer that can be made on a large scale and inexpensively from various materials (Rahman *et al.*, 2021). It has the right biodegradable and edible film-forming qualities (Raeisi *et al.*, 2014). It is a ubiquitous molecule used in preparing drugs and is widely used as an ophthalmic lubricant (Rahman *et al.*, 2021). The excellent biocompatibility, high stability, pH sensitivity, and binding capacity of CMC-based hydrogels, films, or other hybrid materials have attracted much interest in pharmaceutical applications over the last few years, particularly for drug delivery, drug emulsification and stabilization purposes (Adeyeye *et al.*, 2002; Inphonlek *et al.*, 2020; Javanbakht *et al.*, 2020; Maver *et al.*, 2020; Rahman *et al.*, 2021). CMC, an anionic water-soluble biopolymer (structure shown in **Figure 2.5**), has some distinctive properties, such as pH sensitivity, hydrophilicity, nontoxicity, biodegradability, and biocompatibility which made it a promising candidate for nanoparticle modification (Alsaaed *et al.*, 2022). Biomedical fields use CMC and its composites extensively for wound dressing, tissue engineering, bone tissue engineering, biocompatible implant fabrication, 3D-scaffold fabrication, artificial organs or extracellular polymeric matrix mimics, diagnosis, and other applications (Singh *et al.*, 2016; Sadeghi *et al.*, 2020; Sharmila *et al.*, 2020; Rahman *et al.*, 2021; Zheng *et al.*, 2021).

Recent studies indicate that surface modifications using CMC combined with NPs demonstrate greater clinical efficacy than CMC or metal NPs alone. This suggests that the interaction of CMC with NPs enhances their effectiveness, making this approach a promising option for various clinical applications. The synergistic effects observed in these modifications may lead to improved outcomes in treatments and medical devices (Cai *et al.*, 2023). Different research studies have focused on synthesizing nanocomposites that combine CMC with metal-organic frameworks (MOFs). These studies explore the

methodologies involved in creating these nanocomposites, the properties that result from their combination, and potential applications in fields such as drug delivery, environmental remediation, and materials science. By examining the interactions between CMC and MOFs, researchers aim to enhance the functionality and stability of the resulting nanocomposites, making them suitable for innovative applications in technology and industry. **Table 2.2** highlights a summarized overview of CMC-based surface modification of NPs of previous research.

**Table 2.2:** Summarized Studies on CMC-based surface modification of NPs to improve chemical stability and antimicrobial efficacy.

| NPs-Conjugation Studies | Conjugation Outcome | References |
|---|---|---|
| Hydrogel formation by polydopamine, carboxymethyl cellulose, and Ag NPs (PDA-CMC-Ag-NPs) | This innovative PDA-CMC-Ag-NPs composite hydrogel coating can potentially lower infections in catheters and other biomedical devices. | (Cai *et al.*, 2023) |
| CMC edible coating containing Zataria multiflora essential oil and grape seed extract as a food preservative | Attributes to anti-oxidant effect | (Raeisi *et al.*, 2014) |
| CMC and natamycin in active packaging of cheese | Carboxymethyl cellulose-based coatings have doubled the shelf life of high-moisture mozzarella cheese (HMMC). | (Azhdari and Moradi, 2022) |
| Carboxymethyl cellulose/chitosan biguanide hydrochloride edible films activated with frankincense essential oil. | Prepared films exhibited excellent antibacterial activity, especially at a high content of frankincense essential oil (5%) | (Salama, Abdel Aziz and Sabaa, 2019) |
| Edible coating formulation based on carboxymethyl cellulose-silver nanoparticles | Coating formulation significantly ($p<0.05$) inhibited the growth of this fungus as compared to the same coating formulation without coating by silver nanoparticles. | (Jafarizadeh Malmiri *et al.*, 2013) |
| Sodium alginate/CMC films containing pyrogallic acid (PA) | Films with PA, especially at higher concentrations, were more effective against Escherichia coli and Staphylococcus aureus. | (Han and Wang, 2017) |
| Carboxymethyl cellulose-based antibacterial edible coating containing green tea extract. | Inhibition of pecto-bacterium carotovorum-mediated potato soft rot. | (Imm *et al.*, 2024) |

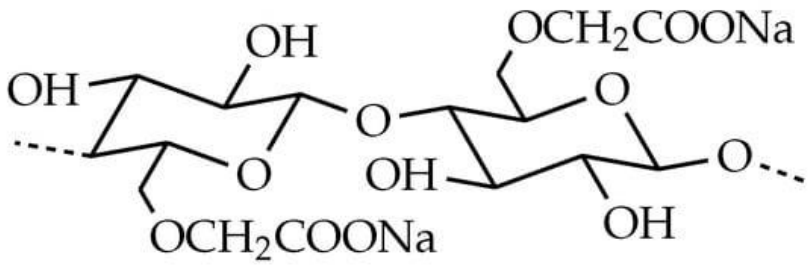


**Figure 2.4:** Structure of CMC which is a cellulose (a fibrous carbohydrate) derivative composed of derivatized glucose joined via β-(1, 4) glycosidic linkages. Reprinted with permission from (Kontogiorgos, 2022).

One of the main obstacles to treating bacterial infection is delivering therapeutic drugs safely, which prevents most medication molecules from bacterial cell walls and uneven distribution to the healthy mammalian cell(Aguilera *et al.*, 2019; Mohsen, Dickinson and Somayaji, 2020). The common adverse effects of the medications used to treat these conditions may be significantly reduced with targeted delivery (Grill and Maganti, 2011; Aguilera *et al.*, 2019; Mohsen, Dickinson and Somayaji, 2020). To address the demand for innovative antimicrobial agents that can adhere to the bacterial cell wall more efficiently than mammalian cells, CMC-loaded ZnO NPs have been prepared and characterized. The mammalian cell is unable to uptake cellulose at the same time; bacteria (such as Lactobacillus) can absorb cellulosic substance or can break cellulosic substance extracellularly by secreting enzymes, which increases the chance of adherence to external cell wall and intracellular distribution (Moraïs *et al.*, 2013; Li *et al.*, 2019; Haokok *et al.*, 2023). ZnO NPs have another superiority over other NPs that might be friendly for biological systems (i.e., antioxidant, anti-inflammatory). ZnO NPs showed considerable antioxidant activity, scavenging 45.47% 2,2-diphenyl-1-picrylhydrazyl (DPPH) at 1mg/mL (Nagajyothi *et al.*, 2015). They also showed remarkable anti-inflammatory action, decreasing iNOS, COX-2, IL-1β, IL-6, and TNF-α mRNA and protein expressions in a dose-dependent manner (Nagajyothi *et al.*, 2015).

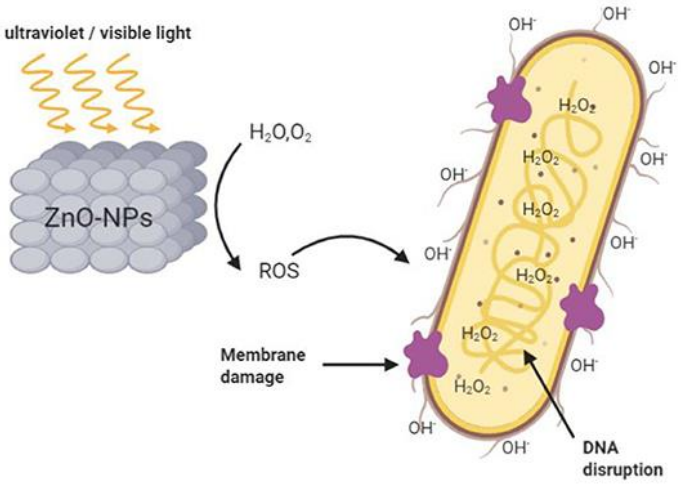


(a) Antibacterial Effect of ZnO NPs by Generating ROS.

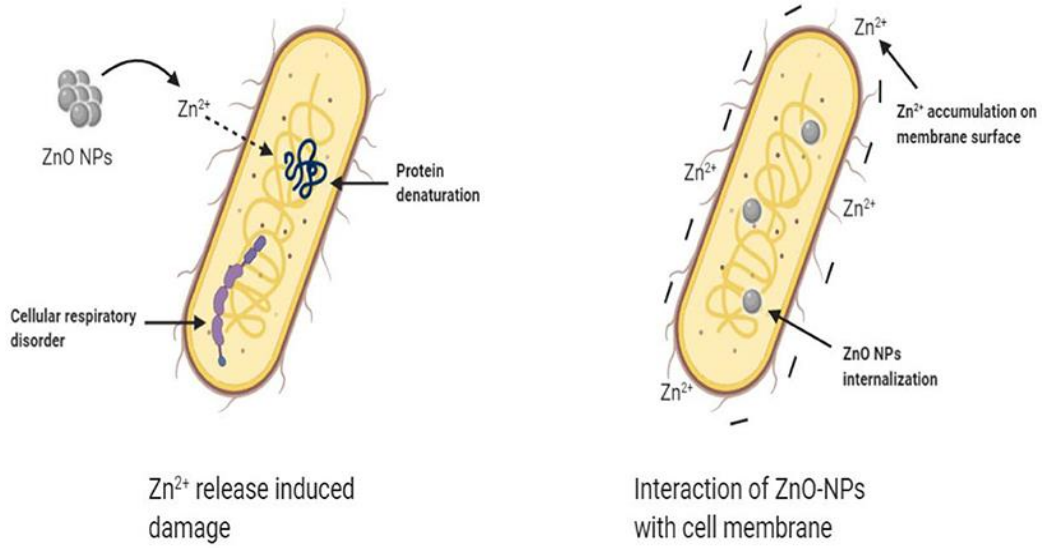


(b) Antibacterial Effect of ZnO NPs by $Zn^{+2}$ release (c) Antibacterial

(c) Effect of ZnO NPs by direct interaction with the cell membrane.

**Figure 2.5:** Mechanism of ZnO-NPs mediated bactericidal effect. (a) Generating ROS by light absorption (b) by releasing $Zn^{+2}$ (c) by direct interaction with the bacterial cell membrane and internalization. Reprinted with permission from (Jiang, Lin and Cai, 2020), *Copyright Frontiers.*

Although various antibiotics are available for treating bacterial infections (including Lactobacillus), finding antibacterial agents with anti-inflammatory and immunomodulatory effects could be a significant milestone in the upcoming antibiotic

resistance crisis (Buret, 2010; Liu, Smith and Rudmik, 2015; Pradhan *et al.*, 2016). The antibacterial mechanism of ZnO NPs has been depicted in **Figure 2.6**.

According to an NCBI PubMed search, 24 studies (from 2013 to 2024) indicate loaded-based nano-composites, hydrogel, and potential applications to various biomedical and clinical applications. As per the studies, none of the studies indicates a preparation method by chemically co-precipitation method and its efficacy. Co-precipitation is the most common surface functionalization method, which is inexpensive and easily replicable (Naz *et al.*, 2020). This study will prepare CMC-loaded ZnO using the technique (Srivastava and Katiyar, 2022). Antibacterial efficacy will be analyzed using a probiotic Lactobacillus culture (Acidophilus and Bulgaricus) from a probiotic culture. Although Lactobacillus is a common non-pathogenic commensal species, the reason behind the choosing of Lactobacillus species is due to its rare pathogenic behavior (bacteremia, endocarditis, cytolytic vaginosis and some evidence in gastric carcinoma) among the elderly and immune-compromised patient (Suresh *et al.*, 2009; Li *et al.*, 2021; Grazioli-Gauthier *et al.*, 2022; Kullar *et al.*, 2023; Ioannou *et al.*, 2024) As predicted, CMC-loaded ZnO NPs could show more potent activity than naïve ZnO NPs and can be utilized as potential antibacterial agents for food packaging (Espitia, Otoni and Soares, 2016; Suo *et al.*, 2017; Copat *et al.*, 2021; Zare *et al.*, 2022; Smaoui *et al.*, 2023) and pharmacological applications.

# CHAPTER 3
# EXPERIMENTAL PROCEDURE

## 3.1 Materials

***ZnO-NPs***

Laboratory grade ZnO NPs of 30 nm size and 99.9 % purity (Density 0.15-0.3 gm/cm$^3$) have been collected from Hebei Suoyi New Material Technology Co. LTD China. The material was initially purchased for research at the Department of Aeronautical Engineering, Military Institute of Science and Technology, Dhaka. A certificate of analysis (COA) has been attached to the supplementary section. Scanning electron microscopic imaging (SEM) of ZnO NPs suggests that experimental ZnO NPs have Length > Diameter in most cases, but many particles are spherical shaped also.

***CMC***

Food-grade CMC, a negatively charged water-soluble polyelectrolyte derived from cellulose, has been sourced from the local market.

***Bacterial Culture Broth***

Lactobacillus MRS broth has been used to expand (Brand: Himedia, Product Code: M369-100G, Origin: India). This medium's composition and performance criteria are per ISO 1995, Draft ISO/DIS 13720:2010 specifications.

***Phosphate buffer saline (PBS)***

The phosphate buffer saline (PBS) source was from Merck (Gibco™,10x). The solution needs to be diluted to ten times before the application. The product is cGMP-compliant under the ISO 13485 standard.

***Bacterial Growth Media***

Lactobacillus MRS Agar has been used as a cultural medium (Brand: Himedia, Product Code: M641l, Origin: India). Its composition and performance criteria are per ISO 1995, Draft ISO/DIS 13720:2010 specifications.

***Bacterial Species***

Lactobacillus species (lactobacillus acidophilus and lactobacillus bulgaricus) have been quantitively extracted from lyophilized probiotics preserved in Fructo-oligosaccharides (Generic Name: GoodGut, Manufacturer: Renata Limited, Origin: Bangladesh). The

product contains Lactobacillus acidophilus (2 billion), Lactobacillus bulgaricus (1 billion), which is a combined 3 billion, and Bifidobacterium bifidum (1 billion).

### 3.2 Equipment

The relevant experiment was conducted at multiple labs of different institutes using different materials and equipment. The preparation and physicochemical characterization by FTIR (Fourier Transform Infrared Spectroscopy) of CMC loaded ZnO NPs was conducted in the Department of Biomedical Engineering, Military Institute of Science and Technology (MIST). Scanning Electron Microscope (SEM) and Energy Dispersive X-ray (EDX) of loaded NPs have been experimented with in the Department of Chemical Engineering, Bangladesh University of Engineering and Technology (BUET), X-ray diffraction (XRD) has been performed at the Center for Advanced Research and Science, University of Dhaka (DU) and Zeta Potentials of the relevant compound has been assessed in Bangladesh Council for Scientific and Industrial Research (BCSIR). The antimicrobial test was performed in the Tissue Engineering lab at the Military Institute of Science and Technology (MIST).

The following equipment has been used throughout the research experiment

- Magnetic stirrer (Biobase, MS7H550-Pro)
- Probe Sonicator (Precisonic, PS-120W)
- Digital Electronic Balance Machine (A&D Company Ltd, Eki 600-3n)
- Biosafety cabinet (Thermo Fisher Scientific, 1300 SERIES A2)
- Centrifuge (Thermo Fisher Scientific, Heracus Multifuge X3R)
- Inverted microscope (Thermo Fisher Scientific, Evos XL Core)
- Autoclave (HYSC, AC-45)
- Oven (Thermostat, OV-H42)
- Anaerobic incubator (Thermo Fisher Scientific, Forma Series 11)
- Petri dish, (SPL Life Science, 90 x 15 mm, crystal grade polystyrene)
- Falcon tube 15 ml and 50 ml (Haier Biomedical)
- Beaker (Schott, duran)
- Scanning electron microscope (SEM) (Zeiss EVO 18)
- Fourier Transform Infrared Spectroscopy (FTIR) (Shimadzu, IR Prestige- 21 PC)
- Particle Analyzer (Malvern Para analytical 3000 Series).

### 3.3 Preparation Method of CMC-loaded ZnO NPs

ZnO NPs functionalization by CMC was done through the co-precipitation method, which used no additional chemicals except the raw materials. **Figure 3.1** depicts the procedure of CMC-loaded ZnO NPs synthesis steps from the relevant raw materials by co-precipitation method. The elaboration of the experimental steps:

**Step 1.** 2.5 gm of dried (Brand Name: A&D Company Ltd. Origin: South Korea) finely ground ZnO NPs were dispersed in 250 mL of demineralized water (DM) and sonicated for 10 min at $35^0$C temperatures by a sonication probe (Brand Name: Cole Parmer, Origin: United States). The pH of the colloidal suspension of ZnO was measured to be 5.96 (2.5gm ZnO dissolved in 250 ml).

**Step 2.** A 0.5% sodium CMC solution was prepared by dissolving 0.25 g of CMC in 250 mL of DM. The pH of the CMC was measured to be 7.06 (0.25 gm dissolved in 250ml). The solution was then mechanically stirred at 1000 rpm (Brand Name: Schengen Hong Fu Scientific Company Ltd. Origin: China) until the complete dissolution of CMC was achieved.

**Step 3.** CMC solution was added dropwise to the ZnO NPs suspension and stirred at 500 rpm for 16 hr.

**Step 4.** The solution was then distributed to a 10 Nos—50 ml falcon tube (Brand Name: Haier Biomedical) and placed in a centrifugation chamber.

**Step 5.** Falcon tubes were placed in a centrifugation device and centrifuged at 1200 rpm for 15 min (Brand Name: Thermo Fisher Scientific, Model: Sorval $^{TM}$ ST8).

**Step 6.** The supernatant was removed. DM resuspended the Falcon tubes again and centrifuged again at 1200 rpm for 15 min.

**Step 7.** The Supernatant was removed again, and pellets were collected from the bottom of all the falcon tubes at the Petri dish.

**Step 8.** Loaded ZnO NPs in Petridis were then dried in an atmospheric oven (Brand Name: Bio-base, Origin: China) at 50 °C for 120 min, which yielded a dried chip and mortared to get finely powdered form of CMC loaded ZnO NPs.

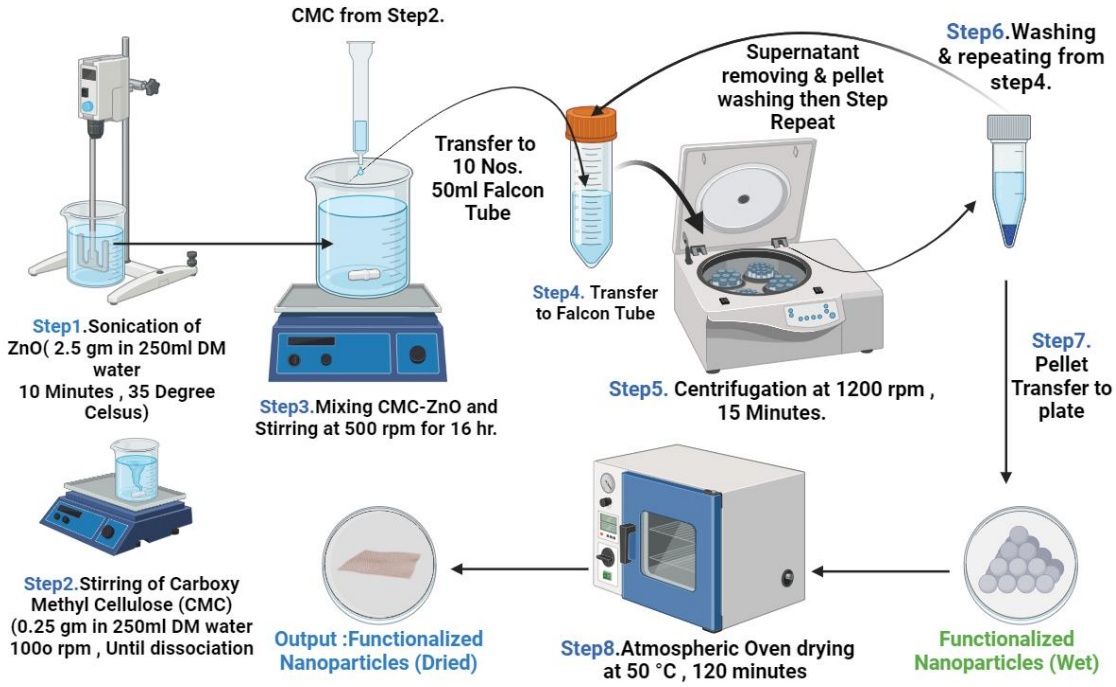


**Figure 3.1:** CMC loaded ZnO NPs synthesis steps from the relevant raw materials by co-precipitation method.

### 3.4 Antibacterial Property Analysis of CMC-loaded ZnO Nanoparticles

***Lactobacillus MRS Agar media preparation***

Lactobacillus MRS Agar was used to grow Lactobacillus species. The media was prepared by suspending 67.15 grams of media bottles and dissolving them in 1000 ml of distilled water. Then, the bottles were heated to a high temperature (near about boiling) to dissolve the medium completely. The media bottles were sterilized by autoclaving at 15 lbs. pressure at 121°C for 15 minutes. The solution was then cooled to 45-50°C and placed in a hot plate to maintain $45^0$ C to prevent solidification before the experiment.

***Lactobacillus MRS broth preparation***

Lactobacillus MRS broth solid was suspended at 55.15 grams in 1000 ml distilled water. Then, the bottles were heated to a high temperature (near about boiling) to dissolve the medium completely. The media bottles were sterilized by autoclaving at 15 lbs. pressure at 121°C for 15 minutes. The solution was then kept to cool down to 45-50°C and poured into 10 Nos—15 ml falcon tubes for bacterial culture addition.

***Dilution of Lyophilized bacteria***

The solution was diluted in isotonic Phosphate buffer saline (PBS) at 10x to prevent cell rupture or fading due to osmosis. Then, the solution was placed at $37^0$ Celsius in an incubator for 30 minutes and diluted by serial dilution up to 3X times to get the cell number 10000/ml. All the dilution was done with 10X PBS solution during the process.

***Transfer of Bacterial Cell to Culture Broth***

0.5 ml of the 3x diluted solutions (10000 Cells/ml) was transferred to the 4.5 ml MRS broth. Eventually, this was 4X dilution. Theoretically, just after adding the bacterial cell, the load of the bacterial cell per ml broth was to be 1000 cells/ml—a total of 20 Nos. The broth had been prepared for further steps. The culture broth is then placed in an Anaerobic incubator at $37^0$ Celsius for four hrs. as the doubling time of Lactobacillus varied from 5.2 hrs. to 9.6 hrs.(Nagpal and Kaur, 2011).

***Sample Labelling and Preparation of Experimental Agents***

The experimental agents (ZnO NPs, CMC, and surface-modified ZnO NPs) at concentrations of 0.1%, 0.5%, and 1.5% were previously measured. They labeled the sample identity as broth and culture plate per **Table 3.1**.

***Immersion of Experimental Agents to Culture Broth and Transfer of Bacterial Culture to MRS agar plate***

Experimental agents were added to the relevant culture broth as per the **Table 3.1.** The time count started once the experimental agents were dipped in bacterial broth solution. After 60 minutes of incubation, 1ml of the broth sterile water was added to the broth (sample No. 1-10) to make the broth volume 10ml from the initial 1ml concentrated solution with concentrated experimental agents. From the diluted broth, 100 μL of the solutions (Theoretically 50 CFU/ml if there is no growth at all; But for maximum growth, it could be up to 75-100 cells/ml, considering the doubling time of Lactobacillus) from the test tubes were transferred to agar plates. MRS agar media was then filled in Petri dishes kept at temperatures between $45^0$ and $50^0$C and swirled three times clockwise and anticlockwise to spread the inoculum on MRS agar media. The thickness of the agar should be roughly 0.3 cm, which was ensured by pouring 15 to 20 ml of media per plate. The

**Table 3.1:** Sample Labelling and Concentration of Experimental Agents.

| Sample No. | Doses Name | Concentration Gm (W/V) |
|---|---|---|
| 1 | Controlled ( NO) | No agents |
| 2 | CMC (N) | 0.1% (0.05) gm |
| 3 | | 0.5%(0.025gm) |
| 4 | | 1.5%(0.075gm) |
| 5 | ZnO NPs (N) | 0.1% (0.05) gm |
| 6 | | 0.5%(0.025gm) |
| 7 | | 1.5%(0.075gm) |
| 8 | CMC loaded ZnO NPs (N) | 0.1% (0.05) gm |
| 9 | | 0.5%(0.025gm) |
| 10 | | 1.5%(0.075gm) |

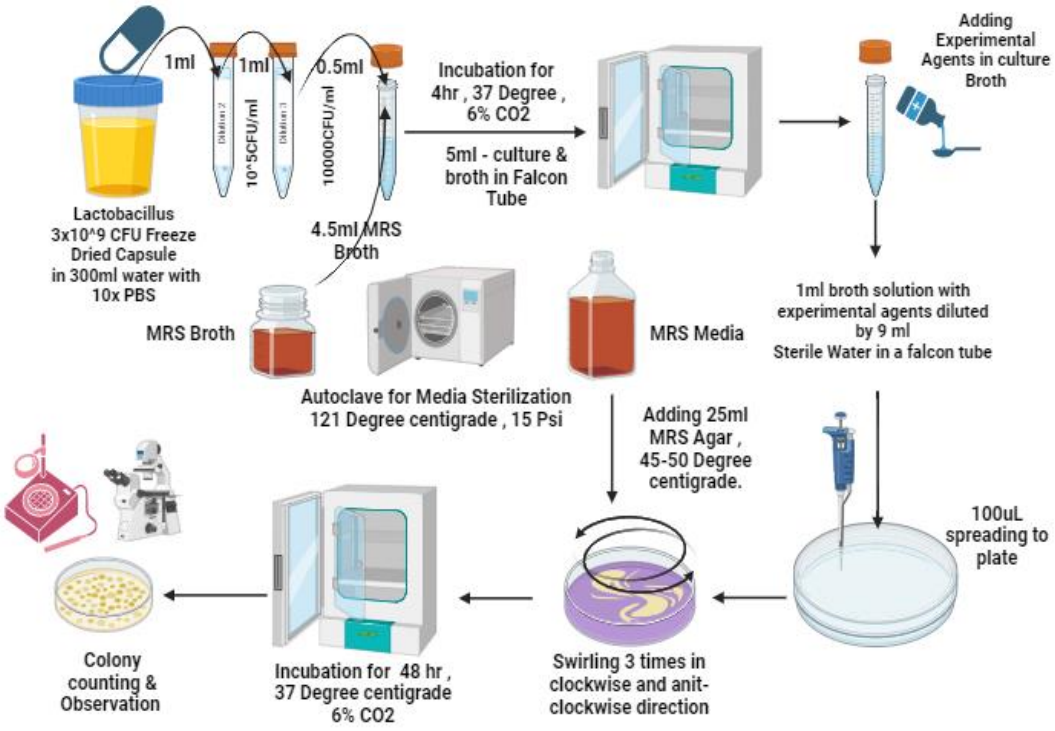


**Figure 3.2:** Process flow chart for adding experimental agents to culture broth and transferring bacterial culture to MRS agar plate.

method applied here was the pour plate method, and the experimental procedure was adopted from (Shadman *et al.*, 2021) and media manufacturer guidelines. Subsequently, all agar plates were incubated at 37 °C for 48-72. hrs. anaerobically in the incubator for final titer count. The overall flowchart of the experimental procedure is explained in **Figure 3.2.**

# CHAPTER 4
# RESULTS AND DISCUSSIONS

## 4.1 Characterization of CMC loaded ZnO NPs

Surface-modified nanoparticles (NPs) were carefully isolated from a centrifuge tube and transferred into a clean Petri dish, as depicted in **Figure 4.1(a).** The NPs were then dried in an atmospheric oven set to a temperature of 50°C for two hours. After this heating period, the dried material formed flakes, which were collected and are shown in **Figure 4.2(b).** Various analytical techniques were employed to fully characterize the flakes' properties. Fourier Transform Infrared Spectroscopy (FTIR) was used to identify functional groups and confirm the surface modification of the NPs. Scanning Electron Microscopy (SEM) provided detailed images that revealed the morphology and size of the flakes. X-ray Diffraction (XRD) analysis helped determine the particles' crystalline structure, while Energy Dispersive X-ray Spectroscopy (EDX) was utilized to analyze the elemental composition. Additionally, Zeta Potential measurements were conducted to assess the stability and surface charge of the nanoparticles in suspension. Furthermore, the antimicrobial activity of the carboxymethyl cellulose (CMC)-loaded zinc oxide (ZnO) NPs was evaluated against Lactobacillus, a species recognized as a beneficial commensal bacterium. This evaluation aimed to determine the modified NPs' effectiveness in inhibiting this microbial strain's growth.

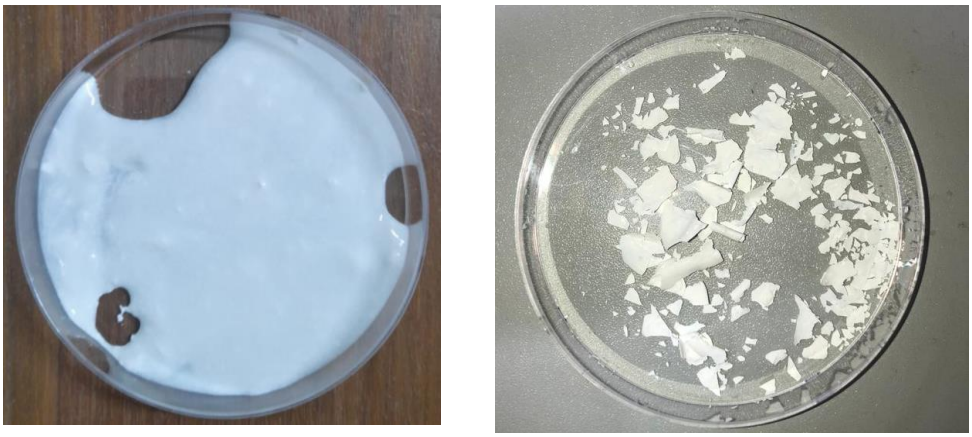

(a) Post Centrifuged (Wet) (b) Post Dried (Dry)

**Figure 4.1:** CMC Loaded ZnO NPs after the development (a) Post centrifuged condition (wet state). (b) Post-drying state (dry).

### *Fourier transform infrared (FTIR) Analysis*

Fourier Transform Infrared Spectroscopy, commonly known as FTIR Analysis or FTIR Spectroscopy, is an analytical method for identifying organic, polymeric, and, in some situations, inorganic materials.(Mattsson *et al.*, 2024). The FTIR analysis method scans test samples using infrared light to determine their chemical characteristics. The FTIR device delivers infrared light ranging from 10,000 to 100 $cm^{-1}$ through a sample, with some absorbed and others passing through. The sample molecules transform the absorbed radiation into rotational and vibrational energy.(Mattsson *et al.*, 2024). The resulting signal at the detector is presented as a spectrum ranging from 4000 $cm^{-1}$ to 400, showing the sample's molecular fingerprint. Each molecule or chemical structure generates a distinct spectral fingerprint, making FTIR analysis an excellent tool for chemical identification (Thill, 2016). Although FTIR analysis is often employed as a qualitative method for material identification, it can also be used quantitatively to quantify certain functional groups if the chemistry is understood and standard reference materials are available. The amount of functionality present in the sample will determine the intensity of the absorbance (Thill, 2016). In this experiment, FTIR analysis was performed, the spectrum is shown in **Figure 4.2** (Brand Name: PerkinElmer, $LiTaO_3$, lithium tantalate MIR detector with an SNR of 9,300:1) for the individual components (CMC and ZnO NPs) and CMC loaded ZnO NPs in the wave number 4000 to 500 $cm^{-1}$. The x-axis—or horizontal axis—represents the infrared spectrum, whereas the y-axis—or vertical axis—represents the amount of infrared light transmitted or absorbed by the analyzed sample material. The absorbance band is typically divided into two regions: (a) Group frequencies, generally above 1,500 $cm^{-1}$, indicating functional groups (i.e., $CH_2$, OH, and C=O). and molecular fingerprint frequencies) (b) fingerprint frequencies, which are highly characteristic of the molecule as a whole, typically seen below 1,500 $cm^{-1.}$ ZnO Molecules has shown the characteristics peak at the region of 3436.55 $cm^{-1}$, 2924.77 $cm^{-1}$, 2854.20 $cm^{-1}$, 1627.53 $cm^{-1}$, 1384.09 $cm^{-1}$, 1019.3 $cm^{-1}$, 873.12 $cm^{-1}$, 5 74.89 $cm^{-1}$, 553.05 $cm^{-1}$, 547.41 $cm^{-1}$ to 526.89 $cm^{-1.}$ The absorption peak at 575.9 $cm^{-1}$ corresponds to metal-oxygen (ZnO stretching vibrations) vibration mode.

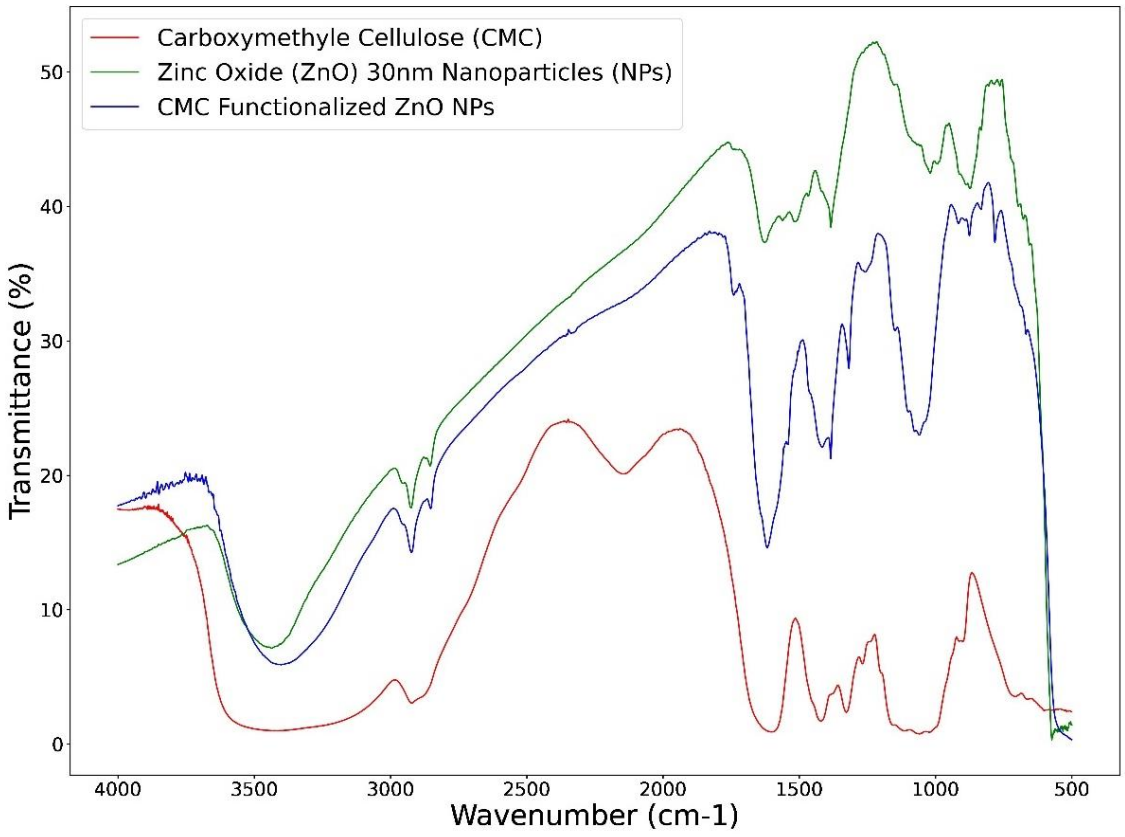


**Figure 4.2:** FTIR Spectrum of CMC (Red Line), ZnO NPs (Green Line), and CMC loaded ZnO NPs (Blue Line).

On the other hand, CMC has shown the characteristic peak at 3420.98 $cm^{-1}$, 2921.95 $cm^{-1}$, 2146.97 $cm^{-1}$, 1602.85 $cm^{-1}$, 1358.18 $cm^{-1}$, 1327.06 $cm^{-1}$, 1058.80 $cm^{-1}$, 900.36 $cm^{-1}$, 707.30 $cm^{-1}$, 601.27 $cm^{-1}$. The vibration bond at 1001 cm-1 can be assigned to the –CH-O-CH2 vibration of ether groups. The vibrational mode peak 1126 can be assigned to the C – O stretching bond vibration. The absorption bands at 1770 cm-1 and 3202 cm-1 are due to C=O and –OH stretching bands, respectively, due to the carboxylic acid group. From the characteristics curve, it was found that the loaded ZnO NPs showed both the characteristics of ZnO and CMC. It can be postulated from the characteristics peak at different points (3401.05 $cm^{-1}$, 2922.79 $cm^{-1}$, 2852.52 $cm^{-1}$, 1739.75 $cm^{-1}$, 1617.99 $cm^{-1}$, 1415.38 $cm^{-1}$, 1384.46 $cm^{-1}$, 1258.60 $cm^{-1}$, 1059.66 $cm^{-1}$, 875.69 $cm^{-1}$, 782.12 $cm^{-1}$) that the loaded molecules have both the characteristics of ZnO and CMC. The wave number for ZnO lies between 2800-3000 $cm^{-1,}$ and for both ZnO & CMC, it lies closely between 1600 $cm^{-1}$ to 750 $cm^{-1}$.

***X-ray diffraction (XRD) Analysis***

X-ray diffraction (XRD) examination was used to determine the nanoparticle's orientation, crystallinity, lattice parameters, purity, and size.(Abraham *et al.*, 2020). It is also used to confirm the phase of NPs (Raja *et al.*, 2022). Each phase creates a distinct diffraction pattern because of the material's chemistry and atomic organization (Raja *et al.*, 2022). The peak positions (2θ values in the XRD pattern) were compared with the International Center of Diffraction Data card (JCPDS), confirming various phases in the produced nanomaterial. The narrow peak in the XRD pattern confirmed the crystallinity of synthesized nanoparticles, and the broad peak in the XRD spectrum indicates the amorphous nature of the material.(Abraham *et al.*, 2020). XRD techniques, widely used in powdered materials after drying their corresponding colloidal solutions, produce statistically representative, volume-averaged findings(Abraham *et al.*, 2020; Raja *et al.*, 2022).

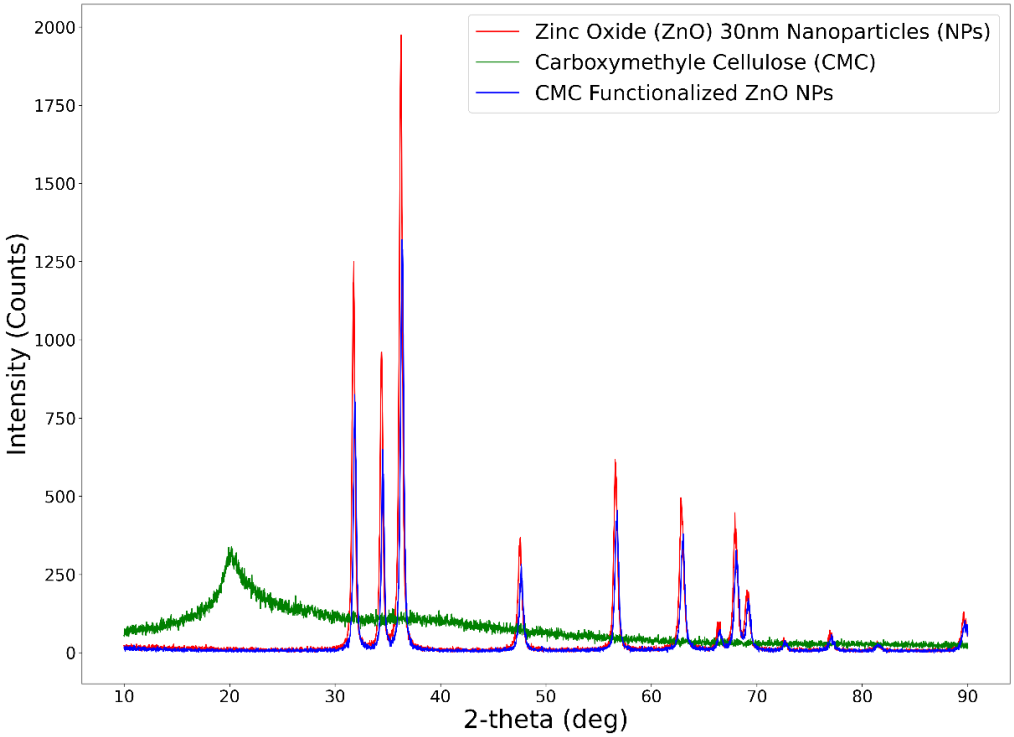


**Figure 4.3:** XRD Spectrum of CMC (Green Line), ZnO NPs (Red Line), and CMC loaded ZnO NPs (Blue Line).

**Figure 4.3** represents the XRD pattern of the CMC-loaded ZnO Nanoparticles. The mean peak of the CMC (green line), ZnO NP of 30nm (red line), and CMC surface-modified

ZnO NP (violet line) suggest that the developed molecules lose a certain amount of CMC from the original molecule and are replaced by ZnO NPs or vice versa. The characteristic diffraction peaks at 2θ values 31.7° (57.49 a.u.), 34.4° (40.54 a.u.), 36.2° (100 a.u.), 47.5° (23.16 a.u.), 56.5° (36.39 a.u.), 62.8° (32.31 a.u.), and 67.9° (26.03 a.u.) confirms the hexagonal crystal structure of ZnO NPs(Bindu and Thomas, 2014). For surface-modified ZnO, the diffraction peaks at 2θ values are 31.8° (56.49 a.u.), 34.5° (37.24 a.u.), 36.3° (100 a.u.), 47.7° (24.01 a.u.), 56.7° (38939 a.u.), 62.9° (35.5 a.u.), and 67.9° (29.49 a.u.). The spectrum of the CMC surface-modified ZnO NPs shows a lower intensity than ZnO NPs in XRD, likely due to the loss of a few atoms from the ZnO crystals. However, the most exciting and revealing insight from the XRD is that the CMC-modified ZnO NPs show X-ray reflection as if they are behaving like crystals (like ZnO NPs) due to the narrower peak(Raja *et al.*, 2022; Tashiro, 2022). Surface loaded ZnO NPs have peaks closely resembling ZnO, although with some molecular replacement. It has sharp peaks at the same angles as ZnO but with a lower intensity. This indicates a homogenous complex that shows crystal characteristics(same as ZnO NPs) in contrast to the amorphous structure of CMC(due to the broader peak)(Raja *et al.*, 2022; Tashiro, 2022).

***Scanning Electron Microscope (SEM) Analysis***

Although FTIR and XRD analysis provided sufficient information about the relevant functionalization (presence of adequate functional group and crystal structure) in the loaded molecule, it didn't give any structural and quantitive information about the precursor and loaded molecule. The scanning electron microscopy (SEM) technique examines the morphology of molecules by scanning the surface with a focused beam of electrons, as well as revealing data about the chemical composition, structure, and orientation of the materials; however, it provides significantly less information about size distribution, actual population, average and cannot distinguish between crystalline and non-crystalline materials (Amidon, Secreast and Mudie, 2009; Paul *et al.*, 2022).

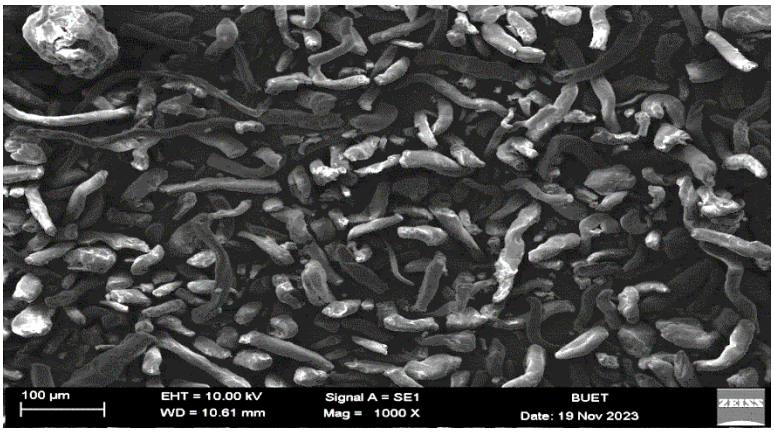


**(a)**

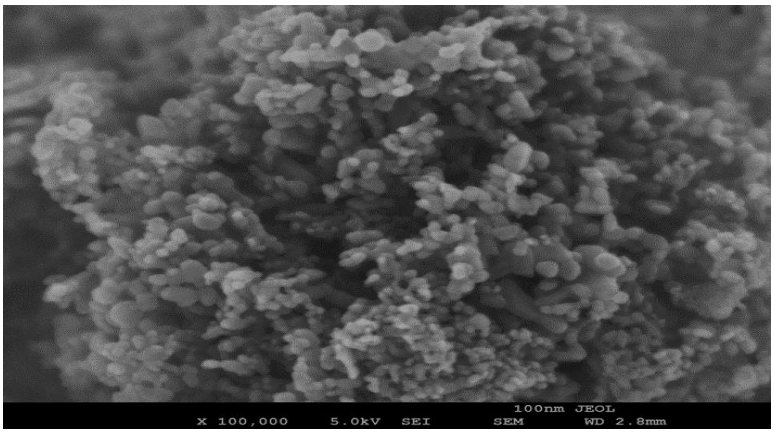


**(b)**

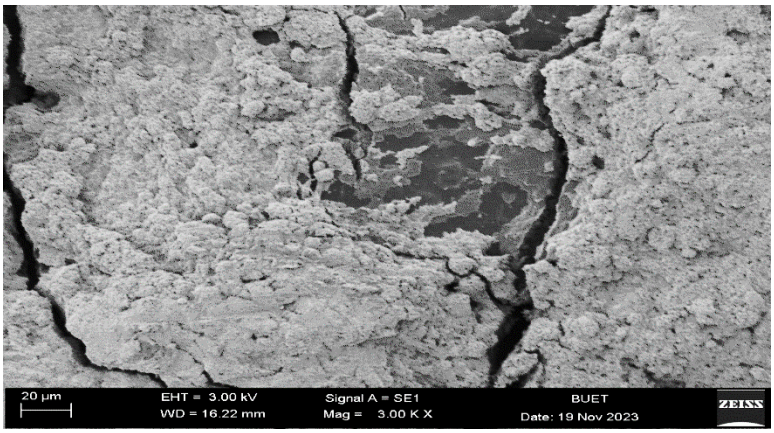


**(c)**

**Figure 4.4:** SEM Imaging of (a) CMC at 10 KV & 1000 times Zoom (b) ZnO Nano-particles, 30 nm at 5 KV and 100,00 times Zoom (c) CMC loaded ZnO Nano-particles at 3 KV and 300,00 times Zoom.

The morphologies of CMC, ZnO, and CMC-loaded surface-modified ZnO nanoparticles (NPs) were examined using a Scanning Electron Microscope (SEM). The CMC-loaded ZnO NPs displayed a well-defined morphology compared to the unmodified CMC and ZnO NPs. **Figure 4.4(c)** presents the structural image of the CMC-loaded ZnO NPs, which differs significantly from the pictures of CMC shown in **Figure 4.4(a)** and ZnO NPs of 30 nm size shown in **Figure 4.4(b).** The uniform distribution of CMC on the surface of the ZnO NPs resulted in a compact, carpet-like integrated structure with a substantial surface area.

***Energy dispersion X-ray (EDX) Analysis of Loaded NPs***

Energy dispersive X-ray analysis (EDX) is carried out with SEM (Roodbar Shojaei, Soltani and Derakhshani, 2022). It offers the elemental specifics of samples near surface elements and the overall positional mapping (Nasrollahzadeh *et al.*, 2019). During EDX examination, an electron beam is carried across the sample to create a picture of the elements present (Nasrollahzadeh *et al.*, 2019). EDX can determine the composition and quantity of heavy metal ions in NPs put near or on the surface of a sample. However, elements with atomic numbers less than 11 are difficult to detect (Roodbar Shojaei, Soltani and Derakhshani, 2022). EDX allows researchers to determine the elemental composition of specific points or map the areal distribution of elements utilizing the electron microscope's scanning capacity(Welker, 2012).

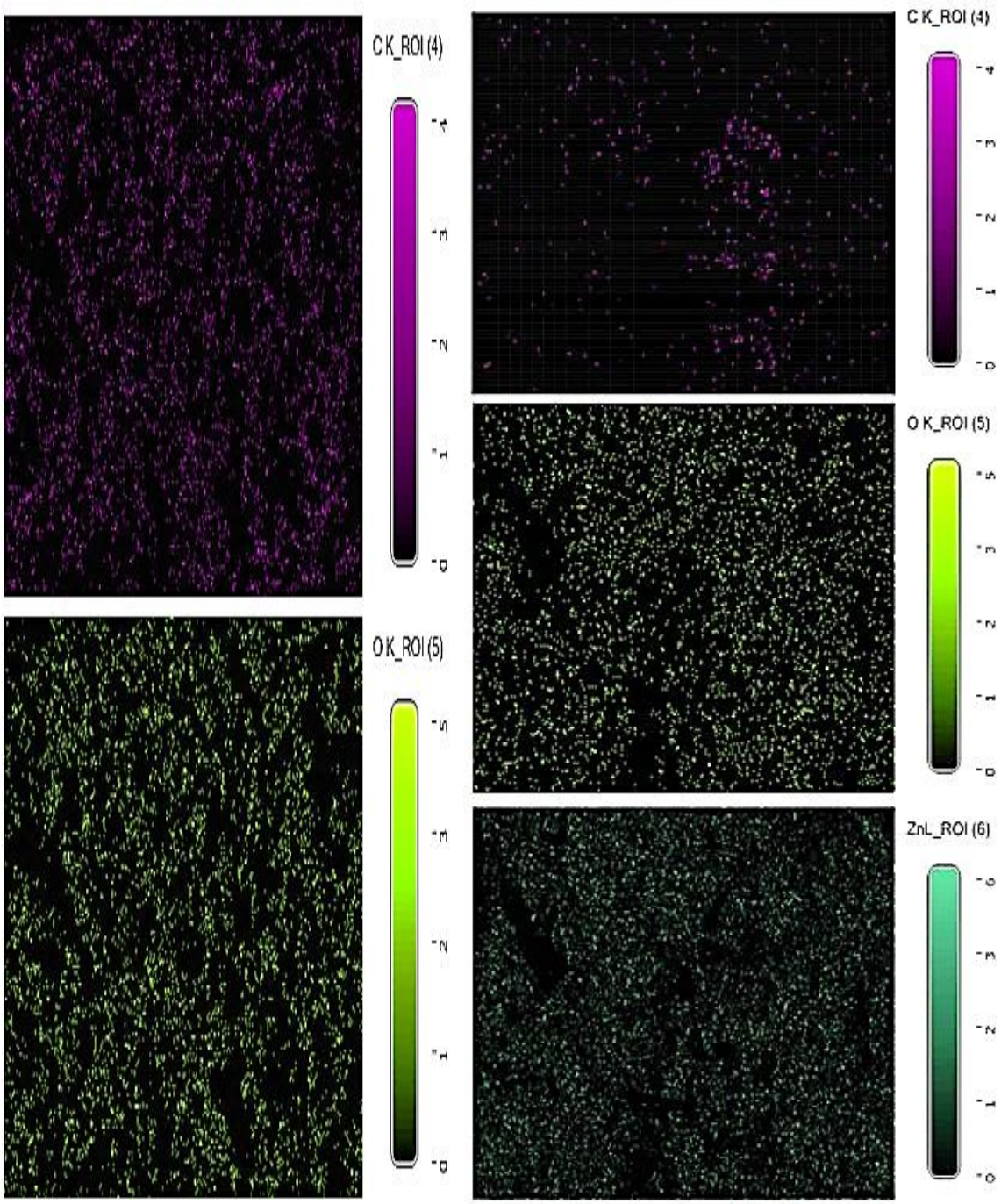


(a) CMC (b) CMC loaded ZnO NPs.

**Figure 4.5:** Molecular Distribution of the CMC loaded ZnO NPs by EDX Mapping (a) CMC (b) CMC loaded ZnO Nanoparticle.

kV: 10 Mag: 1000 Takeoff: 35.5 Live Time(s): 30.7 Amp Time(µs): 3.84 Resolution:(eV) 129.8

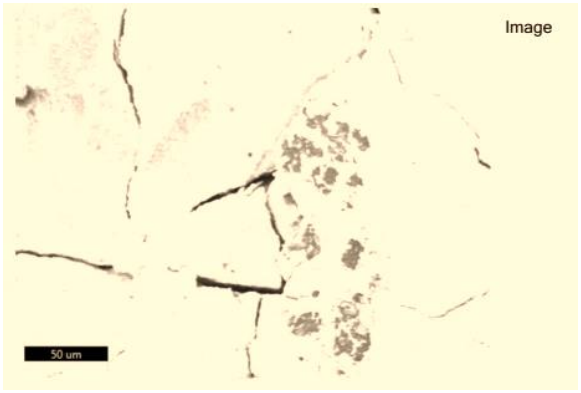


*(a) Image of the selected region for EDX analysis*

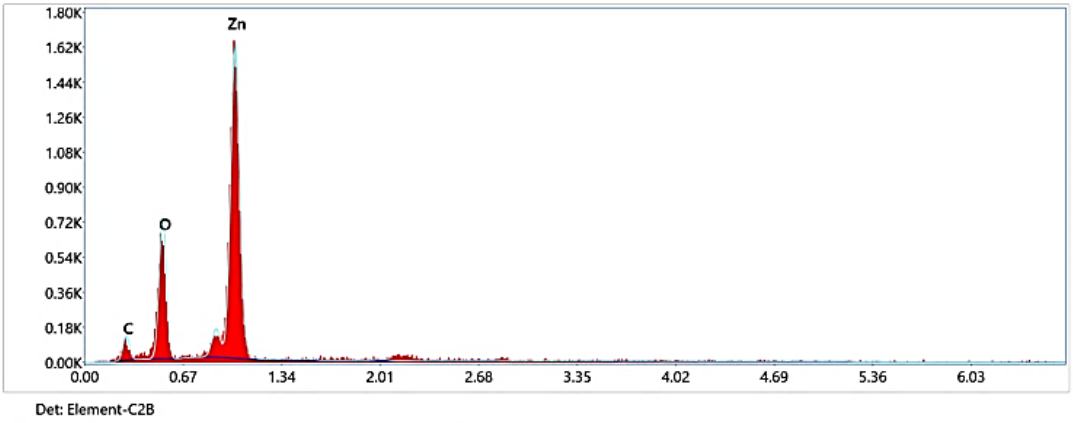


*(b) EDX spectrum analysis of the selected region.*

| Element | Weight % | Atomic % | Net Int. | Error % | R | A | F |
|---|---|---|---|---|---|---|---|
| C K | 10.37 | 26.45 | 22.80 | 15.31 | 0.8314 | 0.1649 | 1.0000 |
| O K | 21.85 | 41.81 | 147.81 | 9.28 | 0.8485 | 0.4256 | 1.0000 |
| ZnL | 67.78 | 31.74 | 290.52 | 6.63 | 0.8683 | 0.6316 | 1.0008 |

(C) *Elemental analysis in the percentage of the selection region from spectrum analysis.*

**Figure 4.6:** EDX Mapping Analysis (a) Image of the selected region for EDX analysis (b EDX spectrum analysis of the selected region (c) Elemental analysis in the percentage of the selection region from spectrum analysis.

| kV:10 | Mag: 1000 | Takeoff: 35.5 | Live Time(s): 10 | Amp Time(µs): 3.84 | Resolution:(eV) 129.8 |
|---|---|---|---|---|---|

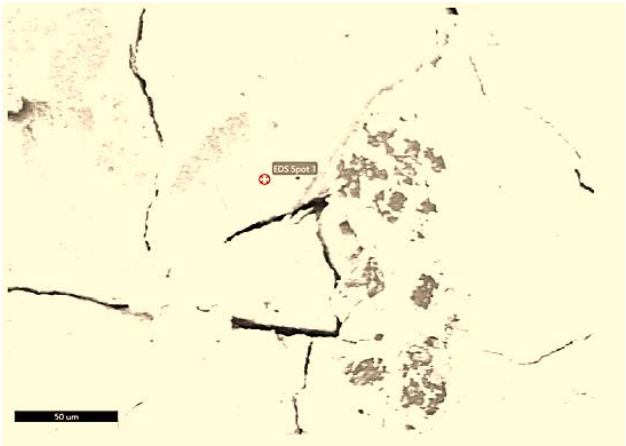


*(a) Randomly Selected Spot from the Flakes at + marked region*

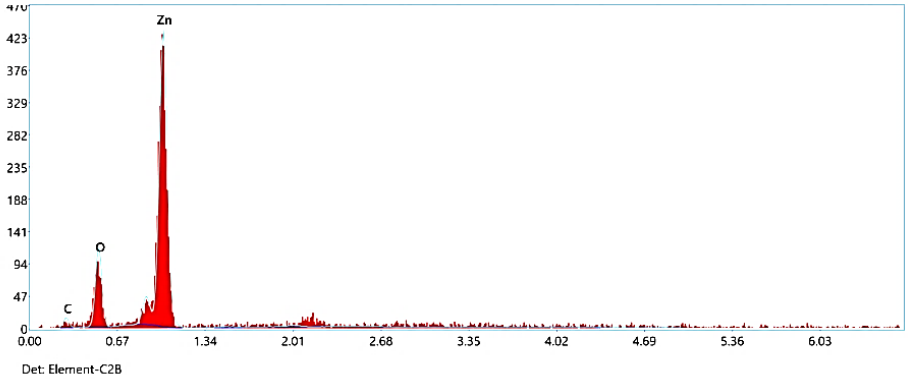


*(b) EDX spectrum of the specific location.*

| Element | Weight % | Atomic % | Net Int. | Error % | R | A | F |
|---|---|---|---|---|---|---|---|
| C K | 5.89 | 18.52 | 8.02 | 26.93 | 0.8120 | 0.1466 | 1.0000 |
| O K | 15.17 | 35.84 | 71.02 | 12.22 | 0.8298 | 0.4218 | 1.0000 |
| ZnL | 78.94 | 45.63 | 240.78 | 7.42 | 0.8505 | 0.6432 | 1.0009 |

*(c) Elemental analysis in the percentage of the specific spot*

**Figure 4.7:** EDX Point Analysis (a) Randomly Selected Spot from the Flakes at + marked region (b) EDX spectrum analysis of the specific location (c) Elemental analysis in the percentage of the selection region from spectrum analysis.

**Figure 4.5** comprehensively shows the elemental distribution profile analyzed through Energy Dispersive X-ray (EDX) spectroscopy. This figure is divided into two parts: **Figure 4.5(a)** illustrates the distribution of elemental components, specifically carbon and oxygen, within CMC matrices. On the other hand, **Figure 4.5(b)** highlights the elemental distribution within CMC matrices that have been incorporated with zinc ZnO NPs, showcasing the presence of carbon, oxygen, and zinc. In **Figure 4.5(a)**, the elemental mapping reveals that carbon and oxygen are integral components of the CMC matrices, indicating their foundational role in the structural composition of CMC. **Figure 4.5(b)** further expands on this by demonstrating that, in addition to carbon and oxygen, zinc has been successfully integrated into the CMC matrix through nanoparticle loading. It is noteworthy that while hydrogen is present in both matrices, it is invisible in EDX analysis due to its low atomic number (Z = 1), which prevents it from generating characteristic X-rays detectable by the equipment (Roodbar Shojaei, Soltani and Derakhshani, 2022). Next, **Figure 4.6** provides insights from the EDX mapping analysis conducted on the CMC-loaded ZnO nanoparticles. The associated X-ray spectrum illustrated in **Figure 4.6(b)** confirms the presence of the three key elements: carbon (C), oxygen (O), and zinc (Zn) embedded within the nanoparticle flakes. Intensity analysis reveals average weight percentages of the elements: carbon comprises approximately 10.37%, oxygen accounts for about 21.85%, and zinc dominates at 67.78%, as detailed in **Figure 4.6(c)**. It is important to reiterate that the hydrogen content has not been quantified in this analysis due to its lack of identifiable X-ray signals (Roodbar Shojaei, Soltani and Derakhshani, 2022). Furthermore, **Figure 4.7** showcases the EDX point analysis, focusing on a randomly selected region of interest within the CMC-loaded ZnO nanoparticles. The X-ray spectrum in **Figure 4.7(b)** corroborates the findings from the mapping analysis, confirming the presence of carbon, oxygen, and zinc within the examined flakes. This point analysis reveals that the elemental distribution within the flakes is neither uniform nor homogeneous. For the specific region analyzed, the elemental weight percentages were found to be 5.89% for carbon, 15.17% for oxygen, and a significant 78.94% for zinc, as shown in the intensity analysis presented in **Figure 4.7(c)**. Once again, it is crucial to note that the hydrogen percentage has been excluded from this assessment due to the absence of characteristic X-rays. Overall, these figures collectively indicate the successful

incorporation of zinc into the CMC matrices, providing vital information about the elemental composition and distribution critical for understanding the functional properties of the CMC-loaded ZnO nanoparticles.

## 4.2 Stability Assessment in Liquid Dispersant

### *Zeta Potential Determination*

The zeta potential quantifies the effective electric charge on the surface of the nanoparticle. (Selvamani, 2019). The concentration of ions with the opposite charge close to the nanoparticle surface screens out charges when a nanoparticle has a net surface charge. (Selvamani, 2019). This layer of ions with opposing charges moves in tandem with the nanoparticle. (Tamrin *et al.*, 2023). The potential difference between the primary fluid in which a particle is disseminated and the fluid layer containing the ions that are oppositely charged and connected to the nanoparticle surface is measured by the zeta potential. (Tamrin *et al.*, 2023). Positive zeta potential particles will attach to negatively charged surfaces and vice versa. Particles with zeta potentials of more than +30 mV or more than −30 mV are usually considered stable. (Gupta and Trivedi, 2018).

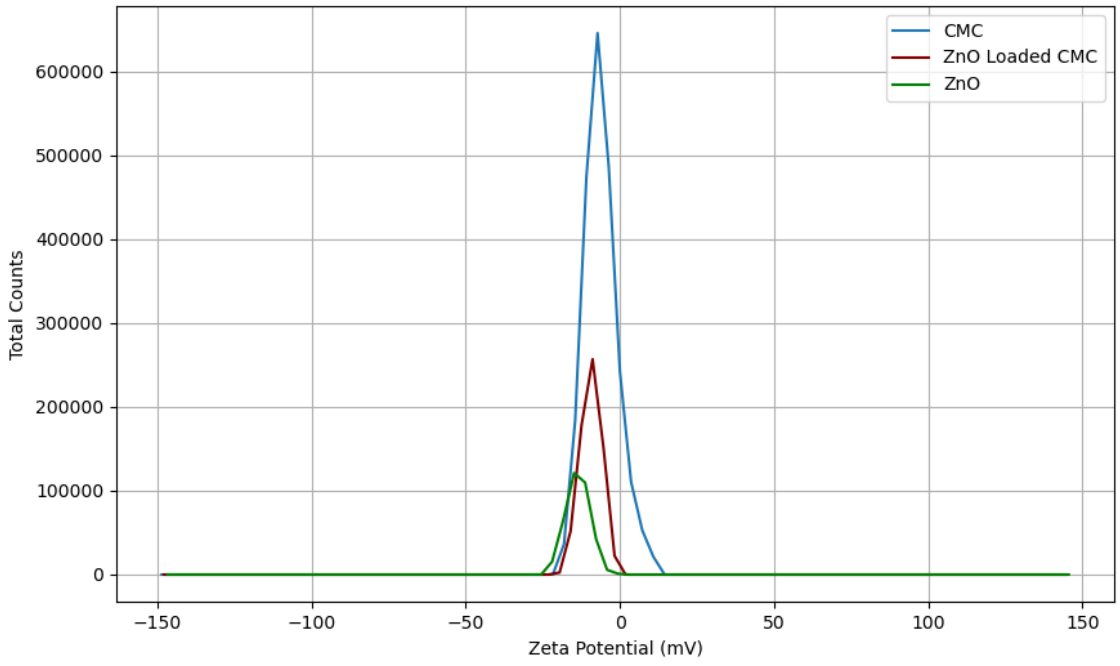


**Figure 4.8:** Zeta Potential of CMC, ZnO NPs, and ZnO Loaded CMC.

From **Figure 4.8**, the mean Zeta potential of the CMC, CMC loaded ZnO NPs, and ZnO NPs were measured (Instrument Brand: Malvern Panalytical, Instrument Serial Number: MAL1232437) in water dispersant (Dispersant Viscosity 0.887 cP, Dielectric Constant: 78.5 and Refractive Index 1.33). The relative zeta potential and conductivity have been represented in **Table 4.1,** which suggests that CMC has higher ionic potentialities than CMC or CMC-loaded ZnO.

**Table 4.1:** Mean Zeta potential and Conductivity Profile of the experimental components.

| Component Name | Zeta Potential (mV) | Conductivity(mS) |
|---|---|---|
| CMC | -6.152 | 0.8218 |
| ZnO NPs | -13.64 | 0.3138 |
| CMC loaded ZnO NPs | -9.348 | 0.3147 |

The relative changes in Zeta Potential showed that CMC-loaded ZnO NPs are unstable in the liquid dispersant. Although the loaded molecule became more positively wall-charged than naïve ZnO NPs, unfortunately, these slight changes couldn't improve the stability of the colloids in liquid dispersion because particles with zeta potentials within +30 mV to −30 mV ranges are considered unstable in liquid dispersant (Gupta and Trivedi, 2018).

### 4.3 Growth Observation and Viability Reduction Analysis

#### *Microscopic observations of probiotic culture*

Probiotic culture (Brand Name: Good Gut, Product of Renata PLC, Bangladesh) containing lactobacillus species (Acidophilus and Bulgaricus) of 3 billion in quantity in fructo-oligosaccharides was diluted to 300ml (with 10 times Phosphate buffer solution to prevent cell rupture) PBS containing sterile water solution. After 30 minutes, a drop of diluted probiotic culture was dipped in the slide (without staining) and observed, as presented in **Figure 4.9**. After staining with methylene blue dye, lactobacillus species (bluish dot) were observed in fructo-oligosaccharides (gel-type structure)(Qian *et al.*, 2020). Lactobacillus species turned blue when stained with methylene blue and observed by an inverted light microscope (Rocha *et al.*, 2014).

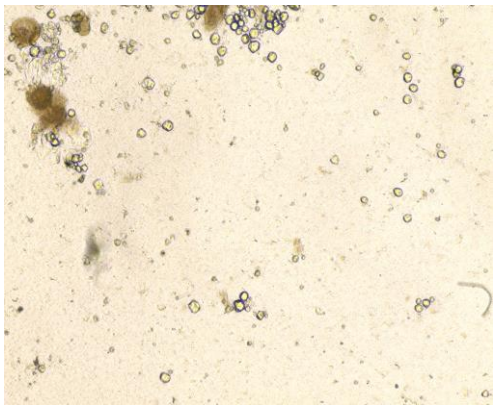

(a) Raw probiotic culture in slide(non-stained)

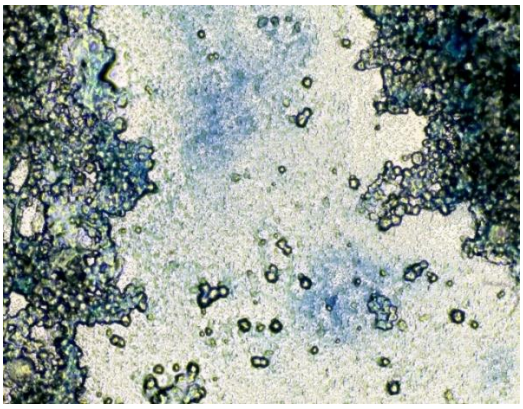

(b) Raw probiotic culture in slide (stained by methylene blue dye)

**Figure 4.9:** Microscopic observations of probiotic culture after 30 minutes soaked in 10 times diluted PBS (a)In a non-stained image (b) stained by methylene blue, Lactobacillus absorbs methylene blue dye(Martínez-Figueroa *et al.*, 2022). The stained blue indicates the presence of lactobacillus immersed in fructo-oligosaccharides.

***Plate observation, colony counting, and viability reduction analysis***

The experimental results obtained from plate counting provided compelling evidence of the effectiveness of the experimental agent in inhibiting the growth of Lactobacillus on MRS agar. As outlined in **Figure 3.2**, the experimental setup involved incubating bacterial specimens treated with various concentrations of the experimental agents for 60 minutes. Sample 1, which served as the control group, was incubated solely with Lactobacillus cultures without adding any experimental agents, acting as a baseline for comparison. In contrast, Samples 2, 3, and 4 were incubated with Lactobacillus culture at 0.1%, 0.5%, and 1.5% (W/V) of CMC, respectively. These varying concentrations allowed for an assessment of the dose-dependent effects of CMC on bacterial growth. Similarly, Samples 5, 6, and 7 were exposed to Lactobacillus cultures at the same concentrations of 0.1%, 0.5%, and 1.5% (W/V), but instead of CMC, they utilized zinc oxide nanoparticles (ZnO NPs) with a diameter of 30 nm. This approach aimed to determine whether the ZnO nanoparticles would exhibit antibacterial properties against Lactobacillus. Samples 8, 9, and 10 were prepared using CMC-loaded ZnO nanoparticles, again at concentrations of 0.1%, 0.5%, and 1.5% (W/V) to further explore the potential synergistic effects. This portion of the experiment was designed to assess how incorporating CMC may enhance

the antibacterial activity of ZnO nanoparticles against the Lactobacillus culture. Following the plating process, all samples were placed in an anaerobic incubator set to maintain a temperature of 37 degrees Celsius and a carbon dioxide concentration of 6% for a total incubation period of 48 hours. This specific environmental condition was critical for the growth of Lactobacillus, as it thrives under anaerobic conditions.

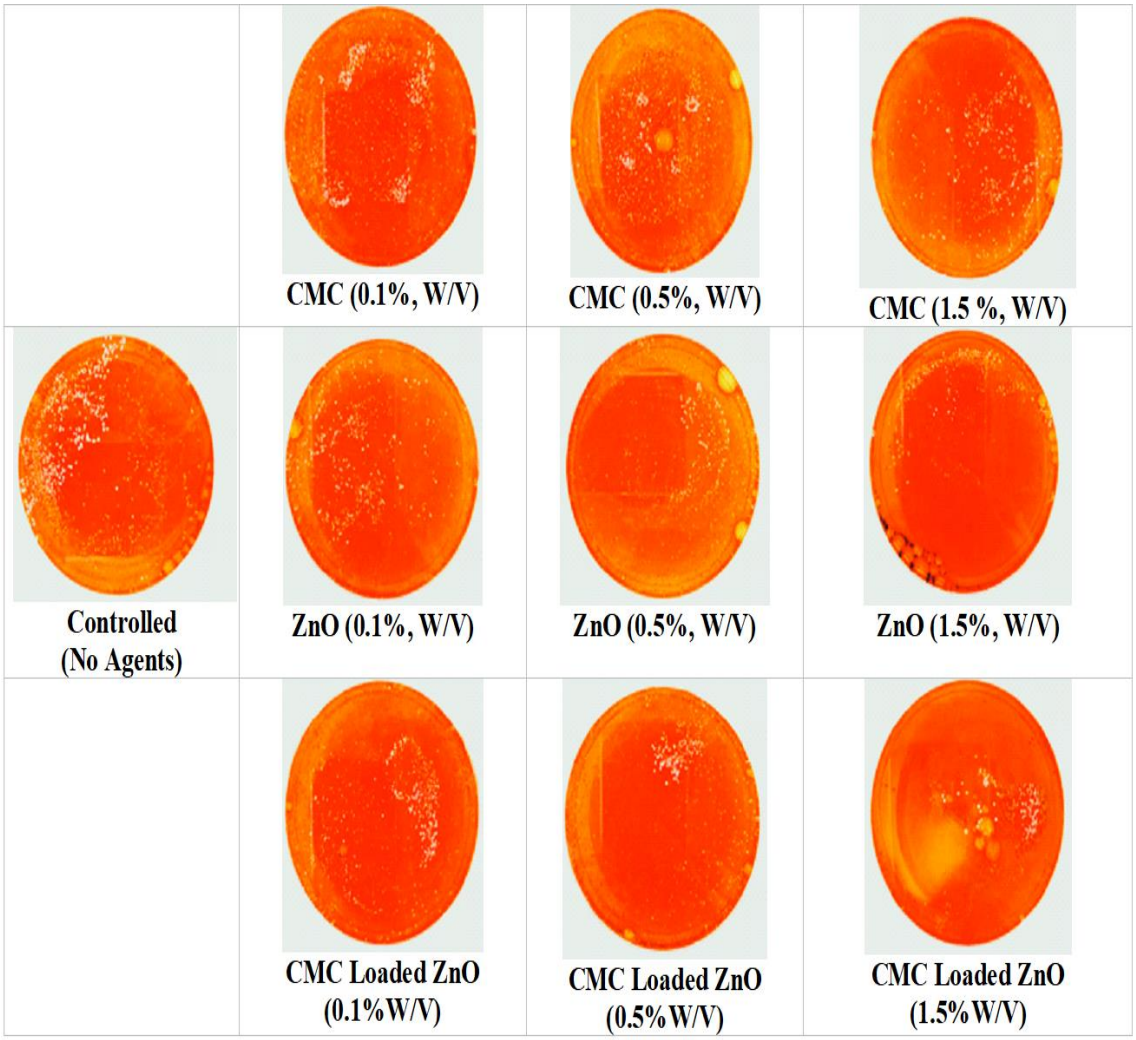


**Figure 4.10:** Observations of Lactobacillus bacterial species growth in MRS agar media at different concentrations of experimental agent.

The experiment, highlighted in **Figure 4.10**, illustrates the effects observed in the incubated plates after the 48-hour incubation period, providing insights into the effectiveness of the various treatments.

**Figure 4.10** illustrates the results of the incubated plate after 48 hours, showcasing the effects of different concentrations of various experimental agents. The observations indicate a clear trend: as the concentration of these agents increases, there is a noticeable inhibition of bacterial growth for both ZnO and CMC-loaded ZnO. This trend is consistent across the different agents tested.

In particular, when CMC is present, bacterial growth is also significantly inhibited; however, it appears this inhibition is not directly proportional to the concentration levels used. CMC is widely utilized in the packaging industry as a viscosity enhancer and bonding agent, but research has also highlighted its antimicrobial properties. According to Ebrahimi et al. (2018), CMC possesses a certain degree of antibacterial activity, although the underlying mechanisms that contribute to these properties are not yet fully understood (Ebrahimi *et al.*, 2018).

ZnO nanoparticles (NPs) are well-established as effective antimicrobial agents. Observations from the experiment reveal that as the concentration of ZnO increases, the inhibition of bacterial growth is markedly more potent than that induced by CMC alone. Furthermore, it is essential to note that CMC-loaded ZnO demonstrates a greater capacity for inhibiting bacterial growth than naïve ZnO; however, this difference becomes insignificant at lower concentrations, specifically at 0.1% w/v. To quantify the degree of growth inhibition, the plate's total colony-forming units (CFUs) were counted using the manual plate count method, which involves a thorough visual inspection of the colonies. The results of this analysis are compiled in **Table 4.2**, providing detailed numerical data on the bacterial growth observed. Moreover, the last column of the **Table 4.2** outlines the percentage reduction in bacterial viability compared to the control sample (which lacked any experimental agents). This viability reduction is further illustrated through graphical representation in **Figure 4.11**, allowing for a more precise visual comparison of the efficacy of the tested agents and concentrations.

**Table 4.2:** Viability reduction analysis from the CFU count.

| Sample No. | Doses Name | Concentration in gm (W/V) | Emersion Time | Plate count (CFU/ml) | Viability Reduction 1-N/N0 × 100% |
|---|---|---|---|---|---|
| **1** | Controlled (N0) | | 60 min | 235.0 | |
| **2** | CMC (N) | 0.1% (0.050gm) | 60 min | 163.0 | 31% |
| **3** | | 0.5% (0.0250) gm) | 60 min | 164.0 | 30% |
| **4** | | 1.5% (0.0750gm) | 60 min | 144.0 | 39% |
| **5** | ZnO NP (N) | 0.1% (0.050gm) | 60 min | 135.0 | 44% |
| **6** | | 0.5% (0.0250) gm) | 60 min | 115.0 | 51% |
| **7** | | 1.5% (0.0750gm) | 60 min | 86.0 | 63% |
| **8** | CMC loaded ZnO NP (N) | 0.1% (0.050gm) | 60 min | 131.0 | 44% |
| **9** | | 0.5% (0.0250) gm) | 60 min | 81.0 | 66% |
| **10** | | 1.5% (0.0750gm) | 60 min | 53.0 | 77% |

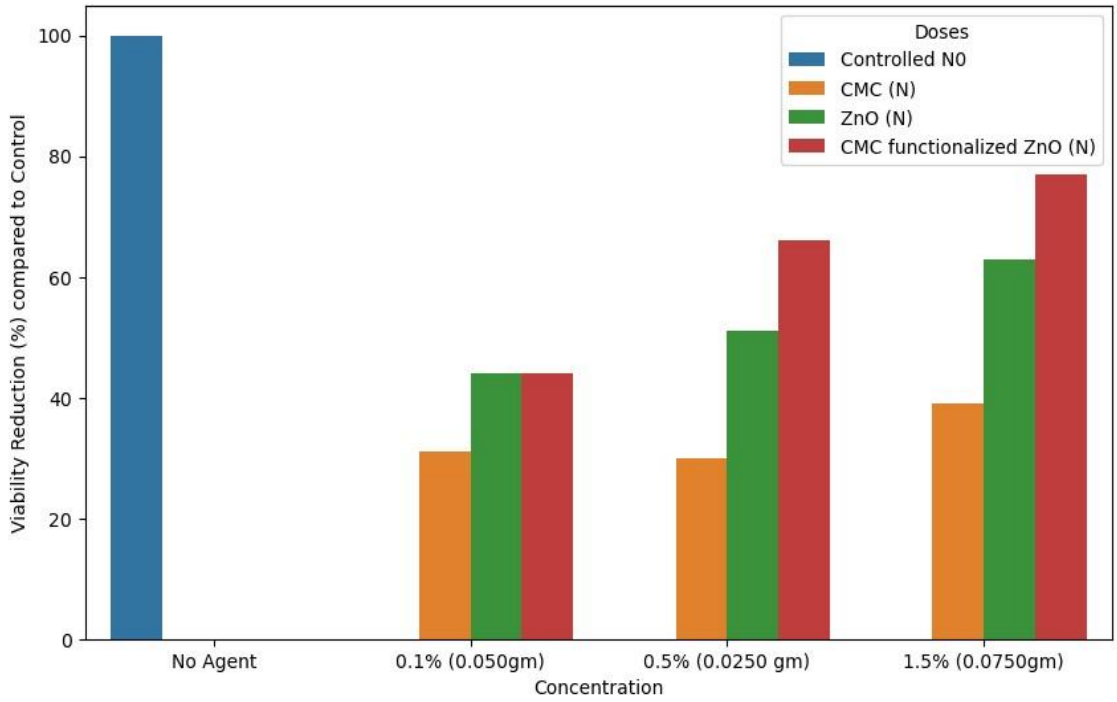


**Figure 4.11:** Graphical presentation of Viability reduction analysis from the CFU count

In these studies, whenever CMC was used alone to assess its antibacterial effect on probiotic culture, it was observed to have some antibacterial effect. The concentration vs. viability reduction studies shows that for 0.1 %, 0.5 %, and 1.5 % of CMC, the relevant reduction rate was 31%, 30% & 39%. The result is quite interesting, as even the cellulosic substance (i.e., CMC) is a certain degree antibacterial. This observation is aligned with previous studies. (Ebrahimi *et al.*, 2018) Where a significant decrease in viability of bacterial cells during 42 days of storage at 25 °C was observed in immobilized edible films based on CMC when ZnO NPs were used at 0.1 %, 0.5 %, and 1.5 % concentration, bacterial viability reduction was observed to be 44 %, 51 % & 63%, respectively. This observation indicates that ZnO is a potent antibacterial. When CMC-modified ZnO NPs were used to assess antibacterial activity at similar concentrations as 0.1 %, 0.5 %, and 1.5 %, bacterial viability reduction was observed to be 44 %, 66 % & 77 %, respectively.

Overall, the observation suggests that a slight modification of ZnO treated by CMC causes an overall increase in antibacterial efficacy at higher concentrations of 0.5% (51% vs 66 %) and 1.5% (63 % vs 77 %).

### 4.4 Potential Mechanism of Action

While Gram-positive and harmful bacteria have a negatively charged cell wall, gram-positive bacteria are considered more resistant to metal NPs, presumably due to the thicker peptidoglycan layer acting as a protective barrier. (Slavin *et al.*, 2017) Cationic nanometals interact with the bacterial membrane, increasing the production of reactive oxygen species and having a mechanical effect on the membrane, which leads to depolarization and cell damage. (Arakha *et al.*, 2015). For example, chemically synthesized ZnO NPs with a positive zeta potential showed high antimicrobial activity at minimum inhibitory concentrations of 50 and 100 mg/L for Gram-negative and positive bacteria, respectively (Arakha *et al.*, 2015).

In this study, CMC-loaded ZnO NPs have shown increased zeta potential (30%) compared to naïve ZnO NPs. This increased zeta potential implies that CMC-loaded ZnO NPs have more surface area and are more stable than naïve ZnO NPs, which makes CMC-loaded ZnO NPs more stable with having more surface area and could interact more with bacterial cell membranes. This increase in zeta potential causes higher antibacterial activity towards gram-positive anaerobic lactobacillus species of two origins (acidophilus and bulgaricus) at the same doses as naïve ZnO NPs. However, in this experiment, zeta potential probably does not influence the antibacterial activity because, in the solution state, zeta potentials of more than +30 mV or more than −30 mV are usually considered stable (Gupta and Trivedi, 2018). Neither of the Zeta potentials falls within the stable ranges required for solution stability.

CMC has a reasonable degree of cellulosic properties (Olukunle, Ayodeji and Akinloye, 2021) When a cellulosic substance loads the surface of a ZnO NP, bacteria might tend to uptake the cellulosic substance (carbohydrate) as part of their nutrient requirements, which ultimately increases the distribution of ZnO NPs inside the cell and causes intracellular damage when ZnO releases ROS or $Zn^{+2}$ as described in **Figure 2.6**. The carbohydrate uptake mechanism of bacterial cells has been depicted as per literature in **Figure 4.12.**

Another hypothesis can be postulated. Bacteria secrete enzymes to break down cellulosic materials for their nutrient requirements (Moraïs *et al.*, 2013; Nurliana *et al.*, 2022). During

the process, CMC-loaded ZnO might break down, and ZnO would have been released closer to the bacterial cell membrane, which might positively impact the bactericidal effect.

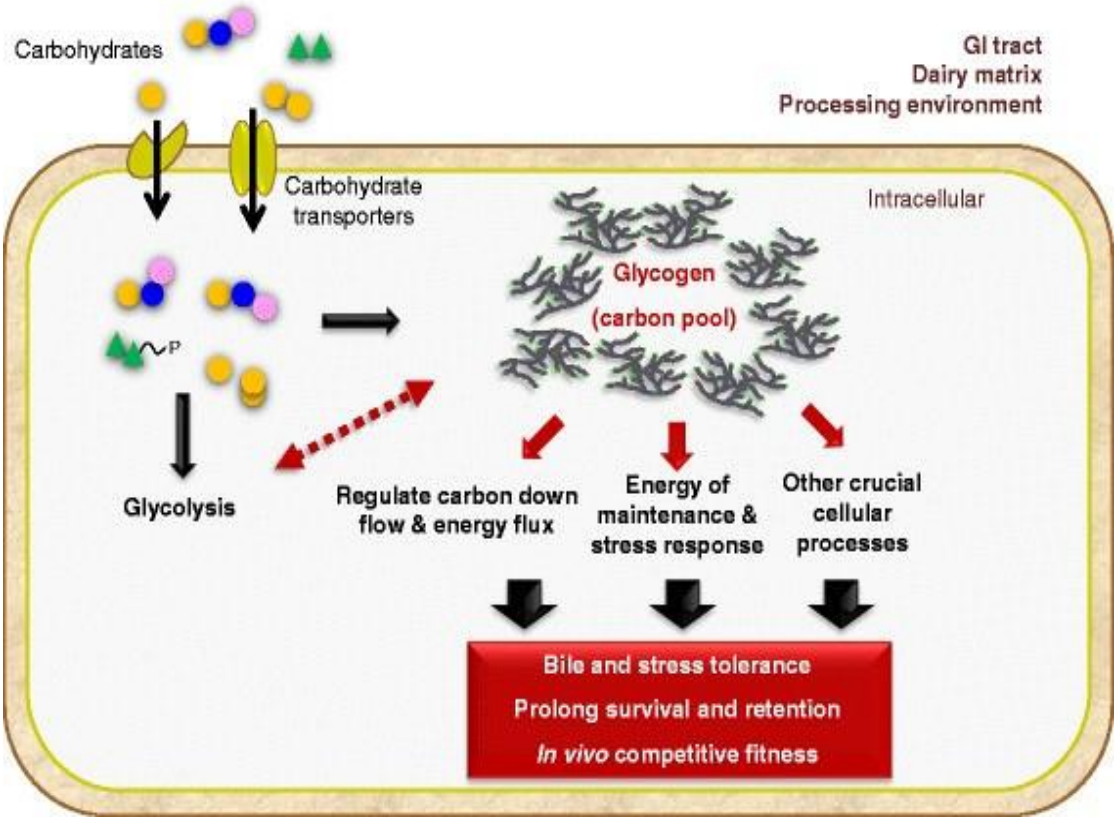


**Figure 4.12:** Potential mechanisms and functions of glycogen metabolic pathway in L. acidophilus. Reprinted with permission (Goh and Klaenhammer, 2014), Copyright: BMC (A part of springer nature).

# CHAPTER 5

# CONCLUSIONS AND RECOMMENDATIONS FOR FUTURE STUDY

## 5.1 Conclusion

- In this investigation, CMC loaded ZnO of 30 nm sizes were developed.
- Chemical properties of CMC loaded ZnO NPs were characterized by FTIR, XRD, SEM, and EDX, where results show the confirmation of CMC loaded ZnO NPs with required chemical and structural change with a 30% increase in the zeta potential towards the positive region but found less stable in solution.
- In an antibacterial susceptibility test against gram-positive anaerobic lactobacillus species, CMC loaded ZnO NPs were found to be relatively more potent antibacterial agents than naïve ZnO NPs at the same external conditions.

## 5.2 Study Limitations

### *Assessment of Mammalian Cell Toxicity*

This study did not test the relevant cellular toxicity of CMC-loaded ZnO NPs against mammalian cells. Although it is well established that CMC is tolerable to mammalian cells (Alsaaed *et al.*, 2022), the outcome when conjugated with ZnO NPs is not predictable. ZnO NPs are generally toxic to mammalian cells due to their inherent ROS-generating capacity.(Sharma, Anderson and Dhawan, 2012). A mammalian cell-specific toxicity study is required before any clinical application.

### *Stability of Loaded Nanoparticles*

The relevant stability of CMC-loaded ZnO NPs was not assessed in this experiment. CMC and ZnO NPs had been required to go through a series of steps during the functionalization process, which might have caused a change to their stability or structure(Desai, 2012). At the same time, the loaded molecule was assessed immediately after preparation for antibacterial studies. The loaded molecule's stability in the longer run is essential, as it might not be stable or broken down. Studies relating to strength and storage conditions are required further. Zeta potential information also suggests that CMC-loaded ZnO NPs are

unstable in a liquid medium. The loaded molecule must be modified further to increase or decrease zeta potential for successive clinical evaluations. (Ernsting *et al.*, 2011; Kędzierska *et al.*, 2021).

***Size and Shape Dependency Study***

In this experiment, ZnO NPs of 30nm and round/slightly oval-shaped have been analyzed. NPs of other sizes and shapes should not be compared with the existing studies as the overall outcome might vary (Søndergaard *et al.*, 2011; Alves *et al.*, 2018).

***Bacterial Strain***

The experiment is only applicable for gram-positive anaerobic lactobacillus species of two origins (acidophilus and bulgaricus) found from probiotic culture. Bacteria of different species or strains of the same species and types (gram-positive or gram-negative, intracellular or extracellular) might behave differently due to their incomparable metabolic behavior (Niu and Zhang, 2023).

**5.3 Scope for future work and possibilities**

CMC-modified ZnO NPs could be used further to investigate as an alternative to bare ZnO NPs due to their increased antimicrobial activities. Apart from the inherent antibacterial potentialities, it can be conjugated with another clinically potential molecule (anticancer, antiviral, antifungal, antibiotics, etc.) by altering the cellulosic bonds to improve the targeted drug delivery medicated by ZnO NPs (Ernsting *et al.*, 2011). Zeta potential data suggest that CMC-loaded ZnO NPs are unstable in a liquid medium. To prevent sedimentation tendency in the solution phase, it is recommended to coat further (i.e., polyethylene glycol or similar molecule) to increase or decrease the zeta potential to make it stable for longer circulation time in blood plasma or biofluids (Kędzierska *et al.*, 2021; Sadalage *et al.*, 2021). More studies are required to be compatible with clinical applications. In this experiment, the research team didn't perform any relevant tests (stability of the molecule, carcinogenicity, mutagenicity, susceptibility towards mammalian cells, and long-term toxicity), which could declare it neither safe nor toxic.

To use CMC-loaded ZnO NPs as an agent for clinical application, some other experiments, such as those on molecule stability, carcinogenicity, mutagenicity, susceptibility to mammalian cells, and long-term toxicity, are required.

# FUNDING AND ACKNOWLEDGEMENT

The project was done per the mandatory requirement for a Master of Engineering degree in Biomedical Engineering. Department of Biomedical Engineering, Military Institute of Science and Technology (MIST), Dhaka, Bangladesh, has provided formal funding for the execution of the project. The author also acknowledges the Bangladesh University of Engineering and Technology (BUET), Bangladesh Atomic Energy Commission (BAEC), and Bangladesh Council for Scientific and Industrial Research (BCSIR) for laboratory support.

## References


Abraham, J., Thajuddin, N., and Mathew, S. (2020). Chapter 2 - Characterization of green nanoparticles from plants. In N. Thajuddin and S. Mathew (Eds.), *Phytonanotechnology*. Elsevier (Micro and Nano Technologies), pp. 21–39.

Adeyeye, M. C., Al-Marhoun, M. A., and Al-Habeeb, F. (2002). Viscoelastic evaluation of topical creams containing microcrystalline cellulose/sodium carboxymethyl cellulose as stabilizer. *AAPS PharmSciTech*, 3(2), p. E8.

Aflakian, F., Shariatinia, Z., and Shamshiri, S. (2023). Nanoparticles-based therapeutics for the management of bacterial infections: A special emphasis on FDA approved products and clinical trials. *European Journal of Pharmaceutical Sciences*, 188, p. 106515.

Afzal, S., Tahir, M., and Adnan, M. (2023). From imbalance to impairment: the central role of reactive oxygen species in oxidative stress-induced disorders and therapeutic exploration. *Frontiers in Pharmacology*, 14, p. 1269581.

Aguilera, G., Gonzalez, P., and Sanchez, J. (2019). Carboxymethyl cellulose coated magnetic nanoparticles transport across a human lung microvascular endothelial cell model of the blood–brain barrier. *Nanoscale Advances*, 1(2), pp. 671–685.

Ai, L., Liu, W., and Zhu, Y. (2019). Polydopamine-based surface modification of ZnO nanoparticles on sericin/polyvinyl alcohol composite film for antibacterial application. *Molecules*, 24(3).

Alsaaed, F. A. T., Hamad, M. A., and Al-Obaidy, K. (2022). Drug delivery system based on carboxymethyl cellulose containing metal-organic framework and its evaluation for antibacterial activity. *Polymers*, 14(18).

Altomare, L., Giuliani, C., and La Rosa, C. (2016). Thermo-responsive methylcellulose hydrogels as temporary substrate for cell sheet biofabrication. *Journal of Materials Science: Materials in Medicine*, 27(5), p. 95.

Alves, T. E. P., Marques, M. B., and Silva, D. R. (2018). Effect of particle shape and size on the morphology and optical properties of zinc oxide synthesized by the polyol method. *Materials & Design*, 146, pp. 125–133.

Amidon, G. E., Secreast, P. J., and Mudie, D. (2009). Chapter 8 - Particle, powder, and compact characterization. In Y. Qiu, G. Zhang, and A. Zhang (Eds.), *Developing Solid Oral Dosage Forms*. Academic Press, pp. 163–186.

Anik, M. I., Mahmud, N., Al Masud, A., and Hasan, M. T. (2022). Gold nanoparticles (GNPs) in biomedical and clinical applications: A review. *Nano Select*, 3(4), pp. 792–828.

Anik, M. I., Mahmud, N., Masud, A. Al, Khan, M. I., Islam, M. N., Uddin, S., and Hossain, M. K. (2022). Role of reactive oxygen species in aging and age-related diseases: A review. *ACS Applied Bio Materials*, 5(9), pp. 4028–4054.

Anjum, S., Abbasi, B. H., and Hussain, I. (2021). Recent advances in zinc oxide nanoparticles (ZnO NPs) for cancer diagnosis, target drug delivery, and treatment. *Cancers*, 13(18).

Antoun, M., El-Charabaty, E., Hadi, M., and El-Sayegh, S. (2020). Uncommon pathogen, *Lactobacillus*, causing infective endocarditis: Case report and review. *Case Reports in Infectious Diseases*, 2020(1), p. 8833948.

Arakha, M., Saleem, M. R., Mallick, B. C., and Jha, S. (2015). The effects of interfacial potential on antimicrobial propensity of ZnO nanoparticle. *Scientific Reports*, 5(1), p. 9578.

Avramescu, M.-L., Decosterd, L. A., and Meyer, S. (2017). Influence of pH, particle size, and crystal form on dissolution behaviour of engineered nanomaterials. *Environmental Science and Pollution Research International*, 24(2), pp. 1553–1564.

Azhdari, S., and Moradi, M. (2022). Application of antimicrobial coating based on carboxymethyl cellulose and natamycin in active packaging of cheese. *International Journal of Biological Macromolecules*, 209.

Babayevska, N., Pokhyl, S., Sukhodub, N., and Solodovnyk, V. (2022). ZnO size and shape effect on antibacterial activity and cytotoxicity profile. *Scientific Reports*, 12(1), p. 8148.

Bindu, P., and Thomas, S. (2014). Estimation of lattice strain in ZnO nanoparticles: X-ray peak profile analysis. *Journal of Theoretical and Applied Physics*, 8(4), pp. 123–134.

Bogdan, J., Pławińska-Czarnak, J., and Zarzyńska, J. (2017). Nanoparticles of titanium and zinc oxides as novel agents in tumor treatment: A review. *Nanoscale Research Letters*, 12(1), p. 225.

Borowik, A., Stolarczyk, E., and Czajkowska, B. (2019). The impact of surface functionalization on the biophysical properties of silver nanoparticles. *Nanomaterials*, 9(7).

Buret, A. G. (2010). Immuno-modulation and anti-inflammatory benefits of antibiotics: The example of tilmicosin. *Canadian Journal of Veterinary Research*, 74(1), pp. 1–10.

Cai, Y., Zhu, Y., and Zhang, Y. (2023). Fabrication of antibacterial polydopamine-carboxymethyl cellulose-Ag nanoparticle hydrogel coating for urinary catheters. *Journal of Biomaterials Applications*, 38(1), pp. 73–84.

Cardoso, D., Silva, P., and Moutinho, A. (2021). Dissolution kinetics of zinc oxide and its relationship with physicochemical characteristics. *Powder Technology*, 378, pp. 746–759.

Copat, C., Manno, E., and Arena, G. (2021). Evaluation of ZnO-NPs in canned seafood by single particle ICP-MS determination. *European Journal of Public Health*, 31(Supplement_3), p. ckab165.283.

Cotton, G. C., Rodriguez, L., and Watson, H. (2019). 3.04 - Antibacterial nanoparticles. In D. L. Andrews, R. H. Lipson, and T. Nann (Eds.), *Comprehensive Nanoscience and Nanotechnology* (2nd ed., pp. 65–82). Academic Press.

Desai, N. (2012). Challenges in development of nanoparticle-based therapeutics. *The AAPS Journal*, 14(2), pp. 282–295.

Ebrahimi, B., Kazemi, R., and Sabaghian, M. (2018). Survival of probiotic bacteria in carboxymethyl cellulose-based edible film and assessment of quality parameters. *LWT*, 87, pp. 54–60.

Ernsting, M. J., Chen, Y., and Wang, H. (2011). Synthetic modification of carboxymethylcellulose and use thereof to prepare a nanoparticle forming conjugate of docetaxel for enhanced cytotoxicity against cancer cells. *Bioconjugate Chemistry*, 22(12), pp. 2474–2486.

Espitia, P. J. P., Otoni, C. G., and Soares, N. F. F. (2016). Chapter 34 - Zinc oxide nanoparticles for food packaging applications. In J. Barros-Velázquez (Ed.), *Antimicrobial Food Packaging* (pp. 425–431). Academic Press.

Fouladi-Fard, R., Mohammadi, A., and Esfahani, N. (2022). The surface modification of spherical ZnO with Ag nanoparticles: A novel agent, biogenic synthesis, catalytic and antibacterial activities. *Arabian Journal of Chemistry*, 15(3), p. 103658.

Gilbert, B., Choi, H., and Lee, S. (2012). The fate of ZnO nanoparticles administered to human bronchial epithelial cells. *ACS Nano*, 6(6), pp. 4921–4930.

Goh, Y. J., and Klaenhammer, T. R. (2014). Insights into glycogen metabolism in *Lactobacillus acidophilus*: Impact on carbohydrate metabolism, stress tolerance, and gut retention. *Microbial Cell Factories*, 13(1), p. 94.

Grazioli-Gauthier, L., Joubert, B., and Melamed, A. (2022). *Lactobacillus jensenii* mitral valve endocarditis: Case report, literature review, and new perspectives. *IDCases*, 27, p. e01401.

Grill, M. F., and Maganti, R. K. (2011). Neurotoxic effects associated with antibiotic use: Management considerations. *British Journal of Clinical Pharmacology*, 72(3), pp. 381–393.

Guerrini, L., Alvarez-Puebla, R. A., and Pazos-Perez, N. (2018). Surface modifications of nanoparticles for stability in biological fluids. *Materials*, 11(7).

Gupta, M., Gupta, S., and Dharmendra, K. (2014). Zinc therapy in dermatology: A review. *Dermatology Research and Practice*, 2014, p. 709152.

Gupta, V., and Trivedi, P. (2018). Chapter 15 - In vitro and in vivo characterization of pharmaceutical topical nanocarriers containing anticancer drugs for skin cancer treatment. In A. M. Grumezescu (Ed.), *Lipid Nanocarriers for Drug Targeting* (pp. 563–627). William Andrew Publishing.

Halbus, A. F., Horozov, T. S., and Paunov, V. N. (2020). Surface-modified zinc oxide nanoparticles for antialgal and antiyeast applications. *ACS Applied Nano Materials*, 3(1), pp. 440–451.

Han, Y., and Wang, L. (2017). Sodium alginate/carboxymethyl cellulose films containing pyrogallic acid: Physical and antibacterial properties. *Journal of the Science of Food and Agriculture*, 97(4), pp. 1295–1301.

Haokok, C., Mahmad, N., and Noor, M. (2023). Efficient production of lactic acid from cellulose and xylan in sugarcane bagasse by newly isolated *Lactiplantibacillus plantarum* and *Levilactobacillus brevis* through simultaneous saccharification and co-fermentation process. *Heliyon*, 9(7), p. e17935.

Hwang, C., Lee, H., and Kim, J. (2022). Reactive oxygen species-generating hydrogel platform for enhanced antibacterial therapy. *NPG Asia Materials*, 14(1), p. 72.

Ikuta, K. S., Suzuki, Y., and Yamamoto, H. (2022). Global mortality associated with 33 bacterial pathogens in 2019: A systematic analysis for the Global Burden of Disease Study 2019. *Lancet*, 400(10369), pp. 2221–2248.

Imm, S., Hwang, S., and Lim, J. (2024). Inhibition of *Pectobacterium carotovorum*-mediated potato soft rot by carboxymethyl cellulose-based antibacterial edible coating containing green tea extract. *Food Science and Biotechnology* [Preprint].

Inphonlek, S., Watanabe, Y., and Takahashi, S. (2020). Chitosan/carboxymethylcellulose-stabilized poly(lactide-co-glycolide) particles as bio-based drug delivery carriers. *Carbohydrate Polymers*, 242, p. 116417.

Ioannou, P., Georgiadou, S., and Karakousis, N. (2024). Infective endocarditis by *Lactobacillus* species—a narrative review. *Antibiotics*, 13(1).

Isık, T., Hilal, M. E., and Horzum, N. (2019a). Green synthesis of zinc oxide nanostructures. In A. M. Nahhas (Ed.), *Zinc Oxide Based Nano Materials and Devices*. IntechOpen.

Isık, T., Hilal, M. E., and Horzum, N. (2019b). Green synthesis of zinc oxide nanostructures. In A. M. Nahhas (Ed.), *Zinc Oxide Based Nano Materials and Devices*. IntechOpen.

Jafarizadeh Malmiri, H., Zolfaghari, B., and Ebrahim, S. (2013). Developing a new antimicrobial edible coating formulation based on carboxymethyl cellulose-silver nanoparticles for tropical fruits and an in vitro evaluation of its antimicrobial properties. *Acta Horticulturae*, 1012, pp. 705–710.

Javanbakht, S., Darvishi, B., and Eskandari, H. (2020). Green one-pot synthesis of multicomponent-crosslinked carboxymethyl cellulose as a safe carrier for the gentamicin oral delivery. *International Journal of Biological Macromolecules*, 164, pp. 2873–2880.

Jiang, J., Pi, J., and Cai, J. (2018). The advancing of zinc oxide nanoparticles for biomedical applications. *Bioinorganic Chemistry and Applications*, 2018, p. 1062562.

Jiang, S., Lin, K., and Cai, M. (2020). ZnO nanomaterials: Current advancements in antibacterial mechanisms and applications. *Frontiers in Chemistry*, 8, p. 580.

Kędzierska, M., Rytel, M., and Kowalski, P. (2021). The synthesis methodology of PEGylated $Fe_3O_4$-Ag nanoparticles supported by their physicochemical evaluation. *Molecules*, 26(6).

Khalaf, M. M., Radwan, H. A., and Said, Z. (2021). Crystalline gold nanoparticles adjusted by carboxymethyl cellulose and citrate salt: Fabrication, characterization, and in vitro anticancer activity. *Journal of Molecular Liquids*, 340, p. 117202.

Khalid, A., Rahman, T., and Naqvi, A. (2021). Synergistic effects of Cu-doped ZnO nanoantibiotic against Gram-positive bacterial strains. *PLOS ONE*, 16(5), p. e0251082.

Kontogiorgos, V. (2022). Stabilisers. In P. L. H. McSweeney and J. P. McNamara (Eds.), *Encyclopedia of Dairy Sciences* (3rd ed., pp. 689–694). Academic Press.

Kullar, R., Hayashi, H., and Gupta, S. (2023). *Lactobacillus* bacteremia and probiotics: A review. *Microorganisms*, 11(4).

Lakshmi Prasanna, V., and Vijayaraghavan, R. (2015). Insight into the mechanism of antibacterial activity of ZnO: Surface defects mediated reactive oxygen species even in the dark. *Langmuir*, 31(33), pp. 9155–9162.

Lakshmipriya, T., and Gopinath, S. C. B. (2021). 1 - Introduction to nanoparticles and analytical devices. In S. C. B. Gopinath and F. B. T.-N. in A. and M. D. Gang (Eds.). Elsevier, pp. 1–29.

Lallo da Silva, B., Borba, P., and Ferreira, T. (2019). Increased antibacterial activity of ZnO nanoparticles: Influence of size and surface modification. *Colloids and Surfaces B: Biointerfaces*, 177, pp. 440–447.

Large, D. E., Rodriguez, S., and Small, K. (2019). Advances in receptor-mediated, tumor-targeted drug delivery. *Advanced Therapeutics*, 2(1), p. 1800091.

Li, W., Gao, X., and Hu, M. (2019). Encapsulation of *Lactobacillus plantarum* in cellulose-based microgel with controlled release behavior and increased long-term storage stability. *Carbohydrate Polymers*, 223, p. 115065.

Li, Y., Liao, C., and Tjong, S. (2020). Recent advances in zinc oxide nanostructures with antimicrobial activities. *International Journal of Molecular Sciences*, 21, pp. 1–70.

Li, Z.-P., Chen, W., and Li, J. (2021). Overgrowth of *Lactobacillus* in gastric cancer. *World Journal of Gastrointestinal Oncology*, 13(9), pp. 1099–1108.

Liao, C., Zhu, D., and Zhang, Q. (2020). Interactions of zinc oxide nanostructures with mammalian cells: Cytotoxicity and photocatalytic toxicity. *International Journal of Molecular Sciences*, 21(17).

Liu, C. C., Smith, T. L., and Rudmik, L. (2015). Oral antibiotics as anti-inflammatories. In P. S. Batra and J. K. Han (Eds.), *Practical Medical and Surgical Management of Chronic Rhinosinusitis* (pp. 237–251). Springer International Publishing.

Luo, M., Zhu, W., and Li, H. (2014). Reducing ZnO nanoparticle cytotoxicity by surface modification. *Nanoscale*, 6(11), pp. 5791–5798.

Mahmud, N., Khan, S., and Alam, M. (2022). Advances in nanomaterial-based platforms to combat COVID-19: Diagnostics, preventions, therapeutics, and vaccine developments. *ACS Applied Bio Materials*, 5(6), pp. 2431–2460.

Makabenta, J. M. V., Nabawy, A., and Li, C. (2021). Nanomaterial-based therapeutics for antibiotic-resistant bacterial infections. *Nature Reviews Microbiology*, 19(1), pp. 23–36.

Mandal, B. K. (2016a). Chapter 9 - Scopes of green synthesized metal and metal oxide nanomaterials in antimicrobial therapy. In A. T. Grumezescu (Ed.), *Nanobiotechnology in Antimicrobial Therapy* (pp. 313–341). William Andrew Publishing.

Mandal, B. K. (2016b). Chapter 9 - Scopes of green synthesized metal and metal oxide nanomaterials in antimicrobial therapy. In A. T. Grumezescu (Ed.), *Nanobiotechnology in Antimicrobial Therapy* (pp. 313–341). William Andrew Publishing.

Martínez-Figueroa, C., Gómez, J., and Flores, A. (2022). One-step staining method for the identification of clue cells and bacterial morphotypes associated with bacterial vaginosis. *Microbiology Spectrum*, 10(3), pp. e01927-21.

Mattsson, K., Broström, L., and Olsson, M. (2024). Chapter 13 - Nanoplastics in aquatic environments—Sources, sampling techniques, and identification methods. In E. Y. Zeng (Ed.), *Microplastic Contamination in Aquatic Environments* (2nd ed., pp. 381–397). Elsevier.

Maver, U., Pavlovic, M., and Kuret, J. (2020). Carboxymethyl cellulose/diclofenac bioactive coatings on AISI 316LVM for controlled drug delivery, and improved osteogenic potential. *Carbohydrate Polymers*, 230, p. 115612.

Mendes, C. R., Pires, R., and Pereira, L. (2022). Antibacterial action and target mechanisms of zinc oxide nanoparticles against bacterial pathogens. *Scientific Reports*, 12(1), p. 2658.

Mohsen, S., Dickinson, J. A., and Somayaji, R. (2020). Update on the adverse effects of antimicrobial therapies in community practice. *Canadian Family Physician*, 66(9), pp. 651–659.

Moraïs, S., Boon, E., and Fernandez, B. (2013). Establishment of a simple *Lactobacillus plantarum* cell consortium for cellulase-xylanase synergistic interactions. *Applied and Environmental Microbiology*, 79(17), pp. 5242–5249.

Murali, M., Jacob, J., and Ramachandran, S. (2021). Plant-mediated zinc oxide nanoparticles: Advances in the new millennium towards understanding their therapeutic role in biomedical applications. *Pharmaceutics*, 13(10).

Nagajyothi, P. C., Choi, M. Y., and Kim, G. Y. (2015). Antioxidant and anti-inflammatory activities of zinc oxide nanoparticles synthesized using *Polygala tenuifolia* root extract. *Journal of Photochemistry and Photobiology B: Biology*, 146, pp. 10–17.

Nagpal, R., and Kaur, A. (2011). Synbiotic effect of various prebiotics on in vitro activities of probiotic *Lactobacilli*. *Ecology of Food and Nutrition*, 50(1), pp. 63–68.

Nasrollahzadeh, M., Sajadi, S., and Akbari, R. (2019). Chapter 6 - Plant-mediated green synthesis of nanostructures: Mechanisms, characterization, and applications. In M. Nasrollahzadeh et al. (Eds.), *An Introduction to Green Nanotechnology* (pp. 199–322). Elsevier.

Navas, D., García, S., and Cornejo, P. (2020). Controlled dispersion of ZnO nanoparticles produced by basic precipitation in solvothermal processes. *Heliyon*, 6(12), p. e05821.

Naz, S., Ullah, H., and Raza, M. (2020). A simple low-cost method for synthesis of SnO2 nanoparticles and its characterization. *SN Applied Sciences*, 2(5), p. 975.

Niu, B., and Zhang, G. (2023). Effects of different nanoparticles on microbes. *Microorganisms*, 11(3).

Nurliana, N., Alvi, A., and Salleh, S. (2022). Identification of cellulolytic lactic acid bacteria from the intestines of laying hens given AKBISprob based on 16S ribosomal ribonucleic acid gene analysis. *Veterinary World*, 15(7), pp. 1650–1656.

Olukunle, O. F., Ayodeji, A. O., and Akinloye, P. O. (2021). Carboxymethyl cellulase (CMCase) from UV-irradiation mutated *Bacillus cereus* FOA-2 cultivated on plantain (*Musa paradisiaca*) stalk-based medium: Production, purification, and characterization. *Scientific African*, 11, p. e00691.

Pandey, J. K., Nema, S., and Sharma, P. (2012). An overview on the cellulose-based conducting composites. *Composites Part B: Engineering*, 43(7), pp. 2822–2826.

Paul, S., Rao, K., and Gupta, N. (2022). Chapter 6 - An overview on nanocarriers. In L. Kumar and Y. Y. Pathak (Eds.), *Nanocarriers for Drug-Targeting Brain Tumors* (pp. 145–204). Elsevier.

Pigłowski, M. (2019). Pathogenic and non-pathogenic microorganisms in the rapid alert system for food and feed. *International Journal of Environmental Research and Public Health*, 16(3).

Pradhan, S., Shrestha, A., and Ghimire, S. (2016). Anti-inflammatory and immunomodulatory effects of antibiotics and their use in dermatology. *Indian Journal of Dermatology*, 61(5), pp. 469–481.

Qian, F., Luo, Y., and Zhang, J. (2020). In vitro study of the antioxidative and antiproliferative capabilities of *Lactobacillus casei* 16-fermented soymilk. *Food Science & Nutrition*, 8(1), pp. 48–57.

Rabin, N., Tzadka, S., and Fishman, A. (2015). Surface modification of ZnO nanoparticles with γ-aminopropyltriethoxysilane and study of their photocatalytic activity, optical properties, and antibacterial activities. *International Journal of Chemical Reactor Engineering*, 14.

Racca, L., Bosetti, M., and Gerosa, M. (2020). Zinc oxide nanocrystals and high-energy shock waves: A new synergy for the treatment of cancer cells. *Frontiers in Bioengineering and Biotechnology*, 8, p. 577.

Raeisi, M., Ghaderi, M., and Zamani, R. (2014). Effect of carboxymethyl cellulose edible coating containing *Zataria multiflora* essential oil and grape seed extract on chemical attributes of rainbow trout meat. *Veterinary Research Forum*, 5(2), pp. 89–93.

Rahman, M. S., Alam, R., and Nahar, N. (2021). Recent developments of carboxymethyl cellulose. *Polymers*, 13(8).

Rasmussen, J. W., Martinez, E., and Louka, P. (2010). Zinc oxide nanoparticles for selective destruction of tumor cells and potential for drug delivery applications. *Expert Opinion on Drug Delivery*, 7(9), pp. 1063–1077.

Reygaert, W. C. (2018). An overview of the antimicrobial resistance mechanisms of bacteria. *AIMS Microbiology*, 4(3), pp. 482–501.

Rocha, T. S., Monteiro, A. A., and Silva, J. L. (2014). Identification and adhesion profile of *Lactobacillus* spp. strains isolated from poultry. *Brazilian Journal of Microbiology*, 45(3), pp. 1065–1073.

Roodbar Shojaei, T., Soltani, S., and Derakhshani, M. (2022). Chapter 6 - Synthesis, properties, and biomedical applications of inorganic bionanomaterials. In A. Barhoum, J. Jeevanandam, and M. K. Danquah (Eds.), *Fundamentals of Bionanomaterials* (pp. 139–174). Elsevier.

Sadalage, P. S., Khot, P. P., and Choudhary, S. B. (2021). Optimally biosynthesized, PEGylated gold nanoparticles functionalized with quercetin and camptothecin enhance potential anti-inflammatory, anti-cancer, and anti-angiogenic activities. *Journal of Nanobiotechnology,* 19(1), p. 84.

Sadeghi, S., Mohammadi, F., and Shafiee, F. (2020). Carboxymethyl cellulose-human hair keratin hydrogel with controlled clindamycin release as antibacterial wound dressing. *International Journal of Biological Macromolecules*, 147, pp. 1239–1247.

Salama, H., Abdel Aziz, M., and Sabaa, M. (2019). Development of antibacterial carboxymethyl cellulose/chitosan biguanidine hydrochloride edible films activated with frankincense essential oil. *International Journal of Biological Macromolecules*, 139.

Sanità, G., Carrese, B., and Lamberti, A. (2020). Nanoparticle surface functionalization: How to improve biocompatibility and cellular internalization. *Frontiers in Molecular Biosciences*, 7, p. 587012.

Scherzad, A., Gehrke, T., and Becker, M. (2017). Molecular mechanisms of zinc oxide nanoparticle-induced genotoxicity. *Materials*, 10(12).

Selvamani, V. (2019). Chapter 15 - Stability studies on nanomaterials used in drugs. In S. S. Mohapatra et al. (Eds.), *Micro and Nano Technologies* (pp. 425–444). Elsevier.

Shadman, S. A., Khan, T., and Patel, A. (2021). Development of a benzalkonium chloride-based antibacterial paper for health and food applications. *ChemEngineering*, 5(1).

Sharma, V., Anderson, D., and Dhawan, A. (2012). Zinc oxide nanoparticles induce oxidative DNA damage and ROS-triggered mitochondria-mediated apoptosis in human liver cells (HepG2). *Apoptosis*, 17(8), pp. 852–870.

Sharmila, G., Aruna, V., and Devi, R. (2020). Fabrication and characterization of *Spinacia oleracea* extract incorporated alginate/carboxymethyl cellulose microporous scaffold for bone tissue engineering. *International Journal of Biological Macromolecules*, 156, pp. 430–437.

Siddiqi, K. S., Ur Rahman, A., and Husen, A. (2018). Properties of zinc oxide nanoparticles and their activity against microbes. *Nanoscale Research Letters*, 13(1), p. 141.

Singh, B. N., Panigrahi, S., and Agarwal, T. (2016). Carboxymethyl cellulose enables silk fibroin nanofibrous scaffold with enhanced biomimetic potential for bone tissue engineering application. *Carbohydrate Polymers*, 151, pp. 335–347.

Slavin, Y. N., Asnis, J., and Häfeli, U. O. (2017). Metal nanoparticles: Understanding the mechanisms behind antibacterial activity. *Journal of Nanobiotechnology*, 15(1), p. 65.

Smaoui, S., Dabbebi, H., and Rebai, H. (2023). Zinc oxide nanoparticles in meat packaging: A systematic review of recent literature. *Food Packaging and Shelf Life*, 36, p. 101045.

Søndergaard, M., Healy, M., and Jensen, K. (2011). Size and morphology dependence of ZnO nanoparticles synthesized by a fast-continuous flow hydrothermal method. *Crystal Growth & Design*, 11(9), pp. 4027–4033.

Srivastava, A., and Katiyar, A. (2022). Chapter 10 - Zinc oxide nanostructures. In K. P. Misra and R. D. K. Misra (Eds.), *Ceramic Science and Engineering* (pp. 235–262). Elsevier.

Suo, B., Xue, Y., and Zhang, L. (2017). Effects of ZnO nanoparticle-coated packaging film on pork meat quality during cold storage. *Journal of the Science of Food and Agriculture*, 97(7), pp. 2023–2029.

Suresh, A., Muni, S., and Singh, R. (2009). Cytolytic vaginosis: A review. *Indian Journal of Sexually Transmitted Diseases and AIDS*, 30(1), pp. 48–50.

Tamrin, S. H., Rahim, H. A., and Chong, H. (2023). Critical considerations in determining the surface charge of small extracellular vesicles. *Journal of Extracellular Vesicles*, 12(9), p. e12353.

Tashiro, K. (2022). Crystal structure analysis by wide-angle X-ray diffraction method. In *Structural Science of Crystalline Polymers: Basic Concepts and Practices* (pp. 1–285). Springer Nature Singapore.

Thill, A. (2016). Chapter 10 - Characterization of Imogolite by microscopic and spectroscopic methods. In P. Yuan, A. Thill, and F. Bergaya (Eds.), *Nanosized Tubular Clay Minerals* (pp. 223–253). Elsevier.

Viswanathan, K., Ramachandran, V., and Rao, S. (2020). Facile approach to enhance the antibacterial activity of ZnO nanoparticles. *Advances in Applied Ceramics*, 119(7), pp. 414–422.

Wang, Y., Zhou, L., and Wu, T. (2023). Antibacterial properties and mechanism of nanometer zinc oxide composites. *Food Packaging and Shelf Life*, 40, p. 101167.

Welker, R. W. (2012). Chapter 4 - Size analysis and identification of particles. In R. Kohli and K. L. Mittal (Eds.), *Developments in Surface Contamination and Cleaning* (pp. 179–213). William Andrew Publishing.

Wisz, G., Podsiadło, P., and Tokarska, D. (2017). Structural, optical and electrical properties of zinc oxide layers produced by pulsed laser deposition method. *Nanoscale Research Letters*, 12(1), p. 253.

Wolfram, J., Kirpotin, D., and Schneider, H. (2015). Safety of nanoparticles in medicine. *Current Drug Targets*, 16(14), pp. 1671–1681.

Yoo, J., Kim, S., and Lee, H. (2019). Active targeting strategies using biological ligands for nanoparticle drug delivery systems. *Cancers*, 11(5).

Youn, S.-M., and Choi, S.-J. (2022). Food additive zinc oxide nanoparticles: Dissolution, interaction, fate, cytotoxicity, and oral toxicity. *International Journal of Molecular Sciences*, 23(11).

Yuan, K., Zhao, X., and Wang, P. (2021). Antibacterial properties and mechanism of lysozyme-modified ZnO nanoparticles. *Frontiers in Chemistry*, 9.

Yung, M. M. N., Tam, K., and Wong, W. (2017). Physicochemical characteristics and toxicity of surface-modified zinc oxide nanoparticles to freshwater and marine microalgae. *Scientific Reports*, 7(1), p. 15909.

Zare, M., Raza, K., and Khan, M. (2022). Emerging trends for ZnO nanoparticles and their applications in food packaging. *ACS Food Science & Technology*, 2(5), pp. 763–781.

Zheng, S., Li, Q., and Zhang, Y. (2021). Gene-modified BMSCs encapsulated with carboxymethyl cellulose facilitate osteogenesis in vitro and in vivo. *Journal of Biomaterials Applications*, 35(7), pp. 814–822.